

RB1904 Cruise Report

Draft 5/28/19

1. Introduction

R/V *Ronald H. Brown* voyage number 1904 is the second of three cruises of an NSF-sponsored project entitled “Shelfbreak frontal dynamics: mechanisms of upwelling, net community production, and ecological implications.” The field work is sited on the continental shelfbreak of the Middle Atlantic Bight, which supports a productive and diverse ecosystem. Current paradigms suggest that this productivity is driven by several upwelling mechanisms at the shelfbreak front. This upwelling supplies nutrients that stimulate primary production by phytoplankton, which in turn leads to enhanced production at higher trophic levels. Although local enhancement of phytoplankton biomass has been observed in some synoptic measurements, such a feature is curiously absent from time-averaged measurements, both remotely sensed and *in situ*. Why would there not be a mean enhancement in phytoplankton biomass as a result of the upwelling? One hypothesis is that grazing by zooplankton prevents accumulation of biomass on seasonal and longer time scales, transferring the excess production to higher trophic levels and thereby contributing to the overall productivity of the ecosystem. However, another possibility is that the net impact of these highly intermittent processes is not adequately represented in long-term means of the observations, because of the relatively low resolution of the *in situ* data and the fact that the frontal enhancement can take place below the depth observable by satellite.

A unique opportunity to test these hypotheses has arisen with deployment of the Ocean Observatories Initiative (OOI) Pioneer Array south of New England. The combination of moored instrumentation and mobile assets (gliders, AUVs) will facilitate observations of the frontal system with unprecedented spatial and temporal resolution (Fig. 1). This will provide an ideal four-dimensional (space-time) context in which to conduct a detailed study of frontal dynamics and plankton communities.

With support from NSF’s Physical, Biological, and Chemical Oceanography programs, we will undertake a set of three cruises to obtain cross-shelf sections of physical, chemical, and biological properties within the Pioneer Array. Nutrient distributions will be assayed together with hydrography to detect the signature of frontal upwelling and associated nutrient supply. We expect that enhanced nutrient supply will lead to changes in the phytoplankton assemblage, which will be quantified with conventional flow cytometry, imaging flow cytometry (Imaging FlowCytobot, IFCB), *in situ* optical imaging (Video Plankton Recorder, VPR), traditional microscopic methods, and HPLC pigments. Zooplankton will be measured in size classes ranging from micro- to mesozooplankton

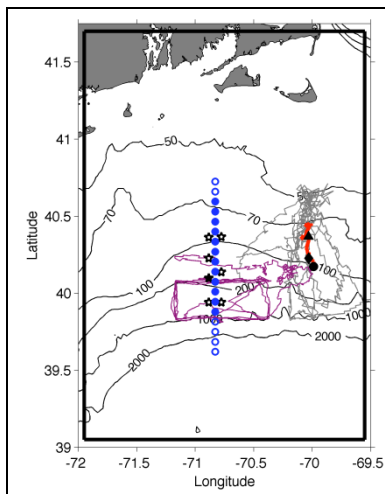
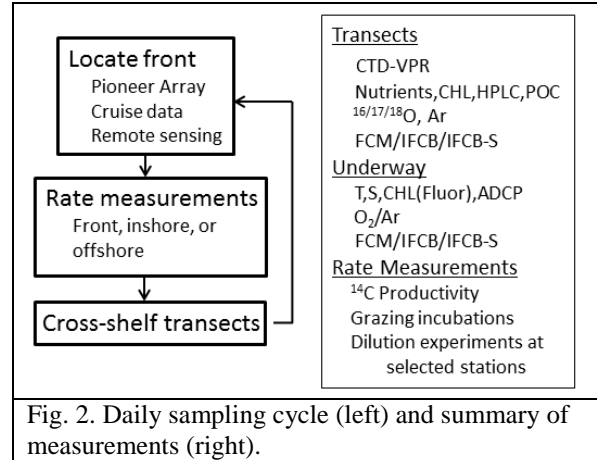


Fig. 1. Tracks of Pioneer Array gliders (grey, magenta lines), 17 Apr – 30 Jun 2014. Red line is a cross-shelf transect on 25-26 Apr; the black triangle, diamond, and circle indicate the positions of the foot, jet and surface expression of the front, respectively. Mooring locations are shown as stars, with the central offshore mooring filled in black. Shipboard transects indicated with blue circles. The solid black boundary depicts our model domain.

with the IFCB and VPR, respectively, and also with microscopic analysis. Biological responses to upwelling will be assessed by measuring rates of primary productivity, zooplankton grazing, and net community production. These observations will be synthesized in the context of a coupled physical-biological model to test the two hypotheses that can potentially explain prior observations: (1) grazer-mediated control and (2) undersampling. Hindcast simulations will also be used to diagnose the relative importance of the various mechanisms of upwelling.



Our observational plan consists of cross-frontal transects and rate measurements, conducted in a daily cycle of activity (Fig. 2). Each day will begin with determining the precise location of the front from a combination of data from the Pioneer Array, cruise observations, and remote sensing images. Rate measurements (¹⁴C and grazing incubations) will be strategically located in one of the three key regimes: inshore, offshore, and at the front. Twelve repetitions of the observational cycle (see below) will permit four replicates in each of the three regimes, facilitating estimates of the mean and variance for each. Each of the 12 cross-frontal transects will consist of a 12-station subset of the range of possible station locations shown in Fig. 2. Each specific 12-station subset will be centered on the front, essentially shifting northward or southward as movement of the front dictates. Station spacing is 7km.

2. Analysis of pre-cruise satellite imagery

On May 7, a large warm core ring was present to the south and east of our sampling area, with low chlorophyll in its interior (Fig 0512.1a). It appears to be entraining high chl water from the shelf into its northeastern flank; high chl is also present to the east and to the west, with a thin filament connecting them along the ring's southern periphery. By May 9, the ring has rotated clockwise, and the shelf entrainment feature is clearly visible in SST (Fig 0512.1b). It has a rather odd shape, with the cold water penetrating linearly NNW/SSE across the NE flank of the ring. Interleaving of warm and cold water masses appear to be associated with a counter-rotating streamer. A warm water outbreak, presumably of ring origin, has entered the southern portion of our line of stations. By 11 May, a tendril of warm water has clearly penetrated the Pioneer Array (Figure 0512.1c). A zoom view shows the detailed structure of that feature (Figure 0512.1d).

3. RB1904 Narrative

Sunday - Monday 12-13 May

Transect 1 completed under challenging weather conditions (Figure 0513.1). The front, as depicted by the 34.5 isohaline, outcrops at station A10, approximately the 130m isobath, where it is a local minimum in chlorophyll. A filament of cold and fresh shelf water is located just offshore of the front, associated with the frontal meander visible in satellite imagery (Figure 0512.1d). ADCP velocities reveal the eastward flow just south of the front (Figure 0513.2).

Incubation cast / MOCNESS tow at A13.

Tuesday 14 May

CDOM sensor removed from CTD, PAR recabled due to faulty connectors.

Incubation casts at A5, A6, A7 to capture replicates of shelf water conditions.

VPR survey A5-A15 (Figure 0514.1). Fishing gear entanglement part way through, resulting in loss of fairing and misalignment of strobe. Images after the gear encounter are not quantitative. Although the fishing gear entanglement disrupted the sampling in the vicinity of the front, the offshore meander is well resolved, with the associated shelf water appearing like a boot-shaped feature in temperature and salinity. The lightest shelf water takes the shape of a surface trapped lens at 39.95N, suggesting the sole and heel of the boot are subducted features. Fluorescence is highest in the offshore waters of the continental slope, and VPR imagery (albeit impaired) appeared to show high abundance of diatom chains (to be confirmed).

Upon completion of the VPR survey, we began a water sampling transect from offshore to onshore.

Wednesday 15 May

Cloudiness has precluded satellite imagery for the last several days, although a recent altimetric analysis confirms the warm core ring to our southeast remains well clear of our sampling area (Figure 0515.1).

Water sampling transect continues; incubation stations at A11 (meander) and A10 (front). Based on the surface salinity of 35.0, station A10 is now on the outside edge of the front in slope water—apparently the front has moved north. By the end of the MOCNESS tow, surface salinity had decreased to 34.5 suggesting arrival at the front. A full water column cast was taken at the zooplankton incubation station to enhance the resolution of the transect. Dramatic evolution of the water mass properties is evident at the front. The 34.5 isohaline shows an inversion, as does the temperature structure in that same vicinity; density is stably stratified, thus indicating subduction at the northern periphery of the front. Chlorophyll remains high inshore of the front, with a local minimum at the front. Highest chlorophyll is located offshore of the frontal filament, which appears to have weakened slightly since the last occupation. Uplift in the density surfaces at station A12 indicates upwelling that locally enhances nitrate concentration where the overlying waters have modest chlorophyll. Highest chlorophyll is found just offshore of that feature where nitrate appears to be most depleted.

Analysis of SST imagery provides some insight into the phenomenology of the developing meander (Figure 0515.2). From May 7 to May 9, the meander begins to roll up on the western side. By May 15, the feature has nearly closed off, apparently on the brink of shedding an eddy. There appears to be leakage of warm slope water emanating westward from the feature along the 200m isobath.

ADCP velocities are consistent with these tendencies (Figure 0515.2, lower panels; 0515.3), including the westward flow of the shelf break jet and eastward flow associated with the rollup meander. Northward migration of the frontal structure is evident (Figure 0515.3), with modest southward movement of the meander rollup.

A MODIS image from 15 May (Figure 0515.4) depicts the high chlorophyll water in the shelf break front rolling up in the eddy-like feature. The filament intersects our sampling pattern from stations A6 to A8, which is consistent with our transect data (Figure 0515.1).

Upon completion of the transect at A5, an underway survey for EIMS analysis was begun:

A5					
EIMS_W1	40	27.9 N	71	2.8	W+
EIMS_E1		40	27.9 N	70	36.6W
EIMS_E2		39	56.7 N	70	36.6W
EIMS_W2	39	56.7 N	71	2.8	W
A18					

Thursday 16 May

Incubation station at A18 to sample slope water conditions. Second incubation cast at A12 to sample the meander filament where uplifted density surfaces appear to be delivering nitrate to near-surface waters (Figure 0515.1).

VPR survey A5-A15 (Figure 0516.1). Optical problems creating ca. 1mm round objects with halo, possible problem with camera alignment. The frontal configuration remains similar to that observed with the prior CTD section (Figure 0515.1). The cold and fresh signature of the meander/eddy feature is no longer evident at the surface, but the subsurface anomalies persist. Satellite imagery shows westward movement of the eddy feature (Figure 0516.2), thus indicating the subducted cold and fresh anomaly persists in the wake of the feature.

Began CTD survey A18-A5.

Friday 17 May

Completed CTD transect. As the meander/eddy feature has moved west, the shelf break front and the shelf-slope front have become occluded: the 34.5 isohaline rises to a local minimum at A11, only to subside offshore and then outcrop at A14 (Figure 0517.1,2). Remnants of the cold and fresh subducted water lie underneath the occluded front, perhaps in a trailing wake of the meander/eddy feature.

Began eddy survey. A dashboard of underway measurements overlaid on the most recent sea surface temperature image helps to guide the sampling (Figure 0517.3). Underway temperature south of the front is slightly colder than indicated in the SST image. However, the temperature gradients line up well, as do the salinity gradients. It is difficult to make sense of the underway fluorometric measurements.

Saturday 18 May

Completed NS section of eddy survey (Figure 0518.1,2). Occlusion of the two fronts has caused the 34.5 isohaline to subside, such that it does not outcrop within the surveyed area. Presumably it outcrops just to the south of the southernmost station in our transect. Chlorophyll is relatively high throughout, excepting the station at the innermost periphery of the occluded front (NS3). EW section began, culminating in a MOCNESS tow at eddy center (NS10). VPR tow eastward to A12, then completed remaining CTDs in the transect westward, finishing at NS4.

The east-west section (Figure 0518.3,4) reveals the signature of eddy center at NS10, with upward doming of the pycnocline and a relatively cold/fresh lens in the upper 40m. The lens is accompanied by the highest surface fluorescence values.

The radial VPR survey from eddy center (NS10) to the edge (A12) also reveals upward doming of the pycnocline at eddy center (Figure 0518.5)

Underway EIMS survey carried out after completion of the CTD survey from NS4 – EW10 – NS13 – NS7 – NS12 – NS10.

Sunday 19 May

Productivity cast at 0600 at eddy center (NS10) followed by productivity and grazing at A12 (front).

VIIRS data from May 18 indicate a broad area of enhanced chlorophyll along the shelf break (Figure 0519.1, left panel). Zooming in on that feature there is patchiness that appears to reflect meander structures, and what could be a relative minimum in chlorophyll associated with the eddy we sampled (Figure 0519.1, right panel). Note that the relative minimum in chlorophyll observed in the VIIRS image is small enough to fit in between our CTD sampling points; radial VPR survey (Figure 0519.2) indicates there could be a local minimum in fluorescence at eddy center.

The VPR survey started at A12 of our standard section, working northward to A5, completing a full N-S transect to the west, and then a partial transect working back north (Figure 0519.2). The survey did not extend far enough west to resample the core of the eddy, but it did capture the trailing meander structure: note that the warm/salty feature to the north of the shelf/slope front is farther north in the central section, which is downstream of the eastern section. Moreover, it appears the warm/salty feature is less distinct in the eastern section, suggesting that merging of the two occluded fronts is nearing completion. In any case, it appears we have captured an event of cross-frontal exchange, which is one of the processes that motivated installation of the Pioneer Array.

The VPR survey documented highest fluorescence at the edge of the inshore front, with high fluorescence extending shoreward. The image data indicated an intense bloom of chain-forming diatoms in the upper 20m at the offshore end of the survey. Curiously, this was not reflected in the fluorescence distribution; perhaps that was a result of non-photochemical quenching.

Underway IFCB measurements detected high abundance of chain-forming diatoms, including *Guinardia*, *Dytilum*, *Chaetoceros*, and other forms. Note this bloom could be associated with the warm water pushing northward in the streamer of the warm core ring, which appears to be entraining water directly from the Gulf Stream (Figure 0519.3).

Transect A5-18 begun.

Monday 20 May

Transect continues, 0600 productivity at A10 (shelf), continue to A13. Transited to A18 for grazing incubation (slope), then worked back to A14 to complete the transect. With the passage of the meander feature, the front has assumed its more traditional cross-shelf morphology, although the temperature, salinity, and density structure shows unusually distinct layering (Figure 0520.1,2). The chlorophyll peak at A12 matches up with the VIIRS image from that same day, suggesting that peak is associated with frontal enhancement in the trough of a meander (Figure 0520.3). The eddy we surveyed is also visible in the image as a ring of chlorophyll surrounding a very small inner core with a local minimum.

Underway EIMS survey sampled the slope water endpoints EIMS_E3 and EIMS_W3

Tuesday 21 May

PP and grazing incubation at A18 (slope).

VPR survey operations were split into two tows because clogging of the ship's sea strainers with salps required a brief period of downtime for maintenance. The combined survey track is shown in Figure 0521.1

VPR survey 5, originating from A18 and proceeding southward, detected a high abundance of rod-shaped diatoms right away from the surface to 40m (Figure 0521.2). Abundance tapered off at ca. 39.5N with the transition to a colder and fresher water mass. We proceeded southward to ascertain whether or not this population would be in the slope water south of the warm core ring streamer (Figure 0521.3). We did not observe high abundance of rod-shaped diatoms, but did notice an increasing number of helical-shaped diatom colonies along the southern periphery of the transect, the eastward extension, and the initial portion of the northward bound leg. We re-encountered high abundance of rod-shaped diatoms on the northbound leg at ca. 39.6N, slightly north of the southern boundary detected on the southbound leg to the west. The high-abundance region extended all the way to ca. 39.8N, the latter portion being overlain by the cold and fresh shelf waters in which abundance was quite low. VPR6 began at A13 and proceeded southward to join the western leg of VPR5. Roughly speaking the high-abundance region of rod-shaped diatoms occupied a similar water mass as the eastern transect, albeit slightly larger in latitudinal extent and shifted to the south.

Began CTD transect at A18 and proceeded northward.

Wednesday 22 May

Transect continues through A8 where productivity and grazing experiments were conducted. Towed VPR south through A18, then returned back to A7 to finish the transect at A5.

VPR survey (Figure 0522.1) reveals a prominent minimum in fluorescence between ca. 40.0 N and 40.1 N; this is also reflected in water mass properties as a cold and fresh lens of low density water. Based on VIIRS satellite imagery, this is a bolus of shelf water entrapped within two adjacent meanders of the shelf break current (Figure 0522.2). IFCB measurements indicate very low numbers of targets in surface underway measurements, thus earning this feature the moniker “desert.” The high abundance of rod-shaped diatoms persists in the waters just offshore of the front, bounded in the offshore direction by the low density lens at the southern periphery of the survey which is presumably associated with the ring streamer. Surface temperatures in this feature are very warm, but relatively fresh; the cause of the latter aspect is not clear. There is also a subsurface titled layer of cold and fresh water at latitude 39.67 (Figure 0522.1), which likely reflects frontal subduction of the shelf water on the onshore edge of the imping warm-core ring, as documented in Zhang and Partida (2018)

Thursday 23 May

Transect completed with productivity station at A5 at 0600. The foot of the front has migrated inshore to A8, and the offshore expression has moved farther offshore to A16 (Figure 0523.1,2). The “desert” identified in the VPR survey (Figure 0522.1) and satellite imagery (Figure 0522.2) is clearly visible in the transect at stations A11 and A12: low chlorophyll, low turbidity, high CDOM, and enhanced nitrate. N.B. step change in nitrate in stations A7-A5 may be due to sensor cleaning.

VPR tow from A5 south to A13/14, turned east then north; aborted due to servo problem. Restarted VPR survey west of the track at NS3, proceeding south to NS5, west to NS11, and north to EW3. The signature of the cold and fresh shelf break eddy appears in present in all sections (Figure 0523.3). The feature appears to have propagated west, with the fluorescence “desert” being most prominent in the NS11-EW3 line. Water mass anomalies are also at a maximum along that line (Cf. Figure 0522.1), and NS4 was identified as eddy center. Note that the warm and salty anomaly at the southeastern extent of the survey was replete with diatoms, consistent with earlier surveys.

Did a MOCNESS tow at eddy center (NS4), followed by a calibration run for the flow meter. The MOCNESS tow at NS4 captured a large amount of salps, and the underway O₂/Ar data shows water in the eddy center is highly heterotrophic. This indicates that the low chlorophyll in the eddy center may be caused by top-down control.

Friday 24 May

0530 MOCNESS tow NS6 eddy periphery/front, which completed the eddy transect (Figure 0524.1,2). The section captures cold and fresh anomaly of the eddy feature, along with its low chlorophyll, high nitrate, and high CDOM characteristics.

Final CTD transect completed (Figure 0524.3,4), indicating the surface expression of the front has migrated slightly shoreward. Nitrate enhanced in the euphotic zone at station A12, indicative of upwelling; battery problems with the sensor at A11, where other measurements show a similar signal to the eddy-induced upwelling described above.

Saturday 25 May - arrival

4. Initial synthesis

Three main themes arise from this initial analysis of our data sets: impact of a warm core ring on the frontal system, blooms of chain-forming diatoms on the offshore side of the front, and upwelling and subduction induced by shelf break meandering and eddy formation. The intense meanders we observed, along with the warm core ring interaction, led to much higher variability in the frontal configuration than we observed in April 2018 (Figure 0525.1).

Warm core ring interaction

A warm core ring to the southeast of our sampling at the beginning of our cruise propagated north and west during our sampling operations. The southernmost periphery of our main transect line was directly affected by a ring streamer by 17 May. Interaction of the ring with the north wall of the Gulf Stream delivered Gulf Stream water northward to just south of our southernmost station, and we did sample that water mass in a VPR survey.

A bloom of chain-forming diatoms on the offshore side of the front

High abundance of rod-shaped chain forming diatoms were observed from offshore edge of the front extending out ca. 10km into the slope waters. The processes leading to this diatom bloom are not clear; hopefully the nitrate and silicate data will provide some clues. It is noteworthy that southern periphery of the diatom bloom was delineated with changing water masses, in some cases associated with the ring streamer complex.

Upwelling induced by shelf break eddy formation

We observed two shelf break eddy formation events, which have revealed a new mechanism for shelf break eddy induced upwelling. In particular, the association of high nitrate and CDOM within the cold and fresh shelf break eddy (Figure 0523.1,2) are indicative of slantwise upwelling of subsurface shelf waters. To visualize the mechanism, consider the mean state of the shelf break current (Figure 0525.2a), in which the surface expression of the front is south of the maximum in velocity. Meanders develop due to instability processes (Figure 0525.2b), and shingle formation is facilitated in northward protrusions of the front into the velocity shear (Figure 0525.2c). As the shingles approach the peak of the downstream meander, anticyclonic shelf break eddies can form (Figure 0525.2d). Next, consider this process in a vertical section through the trough of the meander / eddy center (Figure 0525.3a). As the meander develops, shelf waters are transported southward (Figure 0525.3b). Surface waters are transported laterally, but deeper waters must rise as the shelf waters ride up and over the denser slope waters that lie below the front. As such, high nitrate and high CDOM waters from the deeper part of the

shelf (Figure 0523.1,2) are brought into the euphotic zone. This water mass becomes distinct from its source waters as the meander wraps around the water mass in formation of a shelf break eddy (Figure 0525.2c). In this conceptual model, eddy center is a local minimum in chlorophyll at the time of formation. As the upwelled nitrate is consumed, chlorophyll presumably increases, filling in that local minimum. From that perspective, satellite images such as that shown in Figure 0525.4 suggest the four shelf break eddies are each in a different stage of their life cycle: B, D, C, A from youngest to oldest.

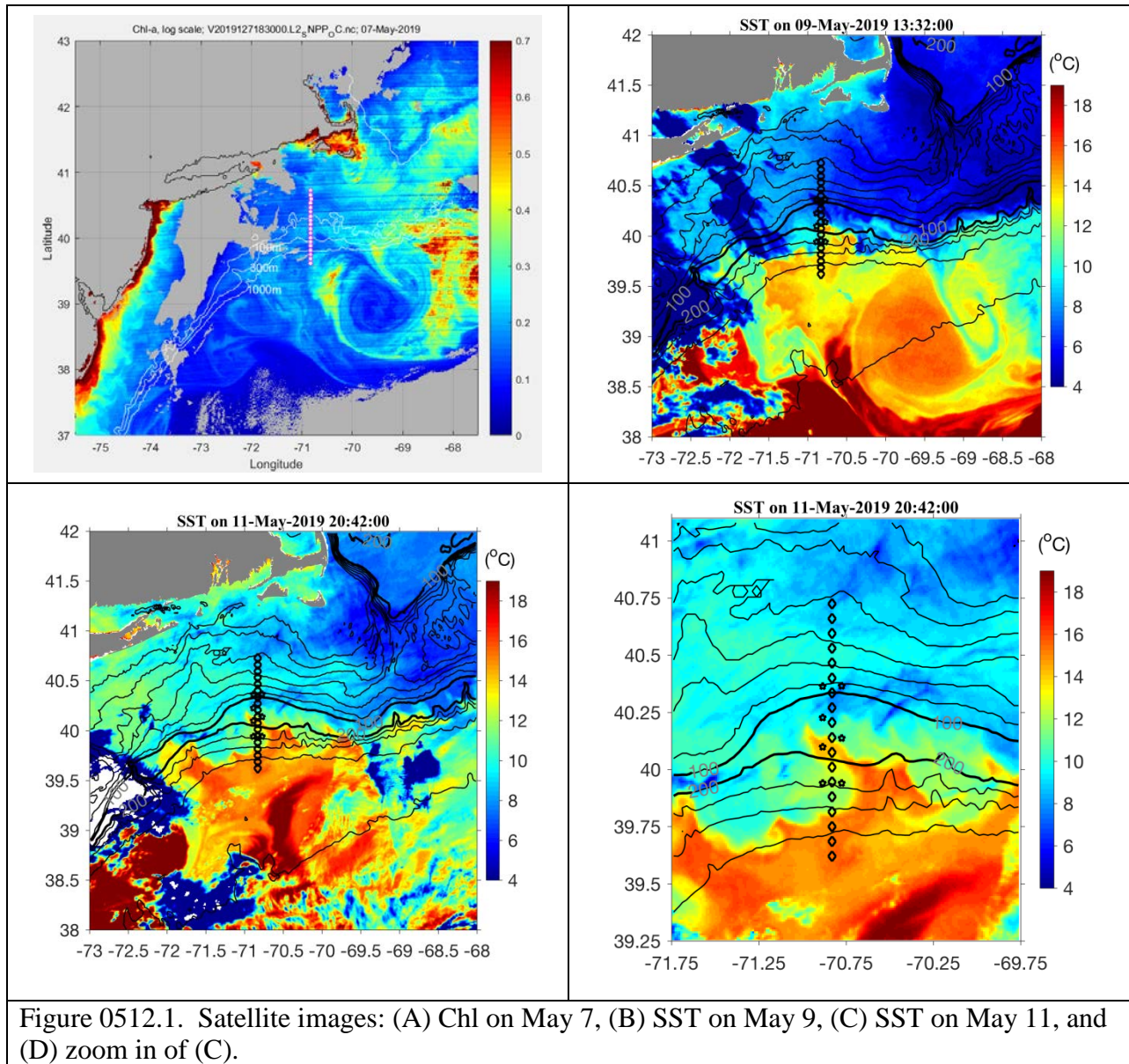
Appendix A. Cruise participants

1	McGillicuddy, Dennis	WHOI
2	Alatalo, Philip	WHOI
3	Hirzel, Andrew	WHOI
4	Eaton, Josh	WHOI
5	Zhang, Gordon	WHOI
6	Xiao, Canbo	WHOI
7	Oliver, Hilde	U Georgia
8	Sandwith, Zoe	WHOI
9	Smith, Walker	VIMS
10	Meyer, Meredith	VIMS
11	Arroyo, Mar	VIMS
12	Lorey, Courtney	College of William and Mary
13	Turner, Jefferson	UMassD
14	Petitpas, Christian	MA DMF
15	Larson, Elizabeth	UmassD
16	dos Santos, Filipe	USP
17	Sosik, Heidi	WHOI
18	Crockford, Taylor	WHOI
19	Connors, Beth	WHOI
20	Bain, Kyra	College of William and Mary
21	Archibald, Kevin	WHOI
22	Luko, Caique	USP
23	da Silva, Felipe	USP
24	Neto, Pedro	USP
25	Chapelle, Phoebe Dreux	ODU
26	Seldon, Corday Rose	ODU
27	Swartz, Marshall	WHOI
28	Black, Allison	NOAA

Date	Morning		
5/13	1100	¹⁴ C, Gr, MOCNESS	A13 shelf / slope
5/14	0700	¹⁴ C	A5 shelf
5/14	0900	¹⁴ C, Gr, MOCNESS	A6 shelf
5/14	1200	¹⁴ C	A7 shelf
5/15	0700	¹⁴ C	A11 slope (meander interior)
5/15	0900	¹⁴ C, Gr, MOCNESS	A10 front (outside edge, in slope water)
5/16	0600	¹⁴ C, Gr, MOCNESS	A18 slope
5/16	1200	¹⁴ C	A12 meander filament / upwelling feature
5/17	0700	¹⁴ C	A12 remnant of meander feature
5/17	1100	¹⁴ C, Gr, MOCNESS	A9 front
5/18	Several	¹⁴ C	Eddy survey
5/18	1500	Gr, MOCNESS	NS10 Eddy
5/19	0600	¹⁴ C	NS10 Eddy
5/19	0800	¹⁴ C, Gr, MOCNESS	A12 front
5/20	0600	¹⁴ C	A10 shelf
5/20	1400	Gr, MOCNESS	A18 slope
5/21	0600	¹⁴ C, Gr, MOCNESS	A18 slope
5/22	1300	¹⁴ C, Gr, MOCNESS	A8 shelf
5/23	0600	¹⁴ C	A5 shelf
5/23	1930	Gr, MOCNESS	NS4 eddy
5/24	0530	Gr, MOCNESS	NS6 eddy periphery / front
Table 1. Incubations.			

Date	Instrument	Start	End	Foot	Surface	Criterion
5/12-13	CTD plus	A5	A15	A8	A10	S=34.5
5/13-14	underway	A15	A5	-	-	
5/14	Incubation casts	A5	A7	-	-	
5/14	VPR 1(note fishing gear entanglement and strobe misalignment)	A5	A18	-	-	
5/14-15	CTD plus	A18	A5	A8	A9	
5/15-16	EIMS survey	A5	A18	-	-	
5/16	Underway / inc casts	A18	A5	-	-	
5/16	VPR 2	A5	A15	-	A10 (11pprox.)	
5/17	CTD plus	A18	A5	A8	A11/A14	
5/17-18	Eddy – NS transect	NS1	NS6a			
5/18	Eddy – EW transect	EW7	A12			
5/18	VPR 3	NS10	A12			
5/18-19	EIMS underway	EW10	NS13			
		NS7	NS12			
5/19	VPR 4	A12	A8			
		NS13	N14			
		NS6A	NS4			
5/19-20	CTDplus	A5	A18	A9/10	A15	
5/20-21	EIMS underway	A14	A16			
		EIMS_E3	EIMS_W3			
		A16	A18			
5/21	VPR 5 + 6	See text				
5/22-23	CTD plus	A18	A8 /A5	A8/A9	A16	
5/22	VPR 7	A8	A18 plus			
5/23	VPR 8	A5	A13/A14			
		3.8nm E	North			
5/23	VPR 9	NS3	NS5			
		NS11	EW3			
5/23-4	CTD plus	NS3	NS6	-	-	
5/24	CTD plus	A18	A8		A15/A16	

Table 2. Transects and frontal locations based on the criteria indicated in the right-hand column. Estimates based on data that did not quite reach the surface or bottom indicated by asterisks.



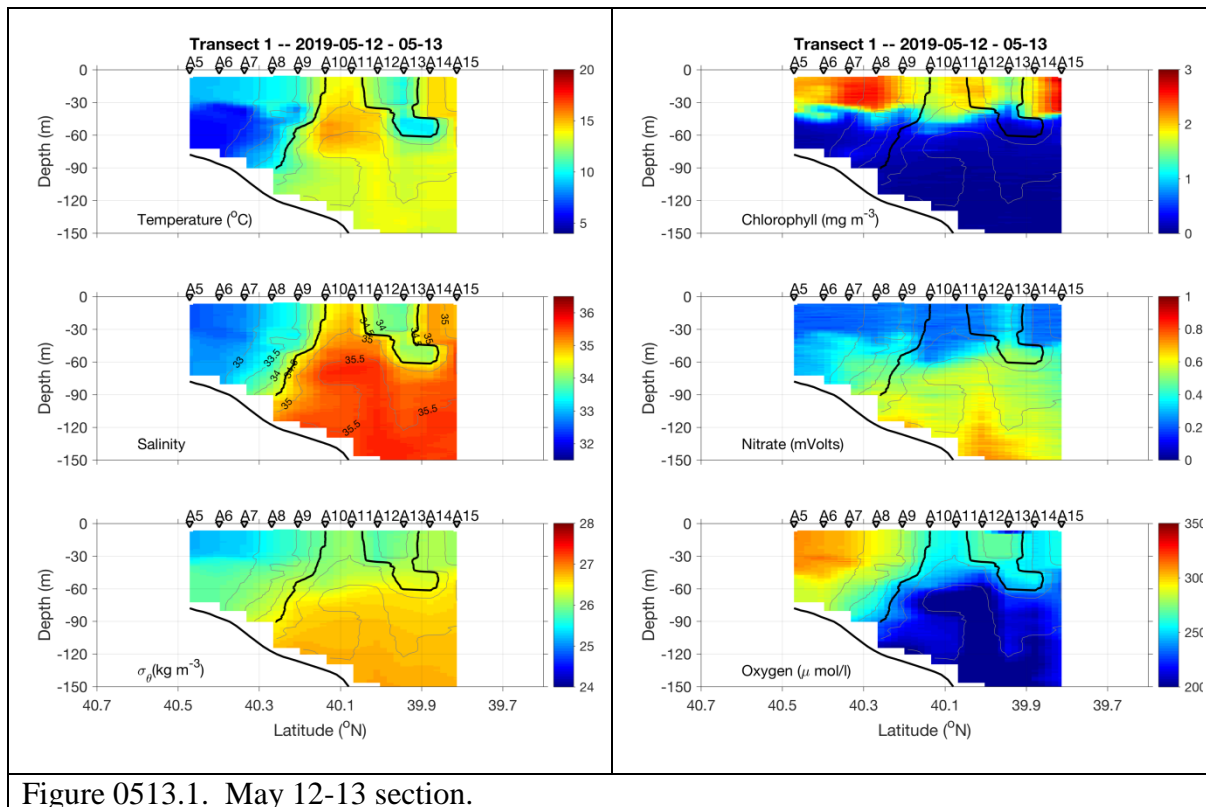


Figure 0513.1. May 12-13 section.

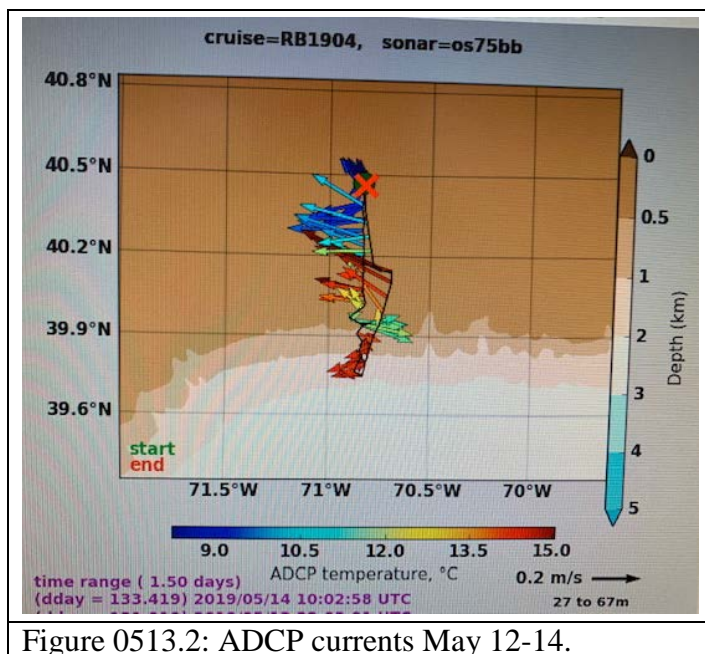


Figure 0513.2: ADCP currents May 12-14.

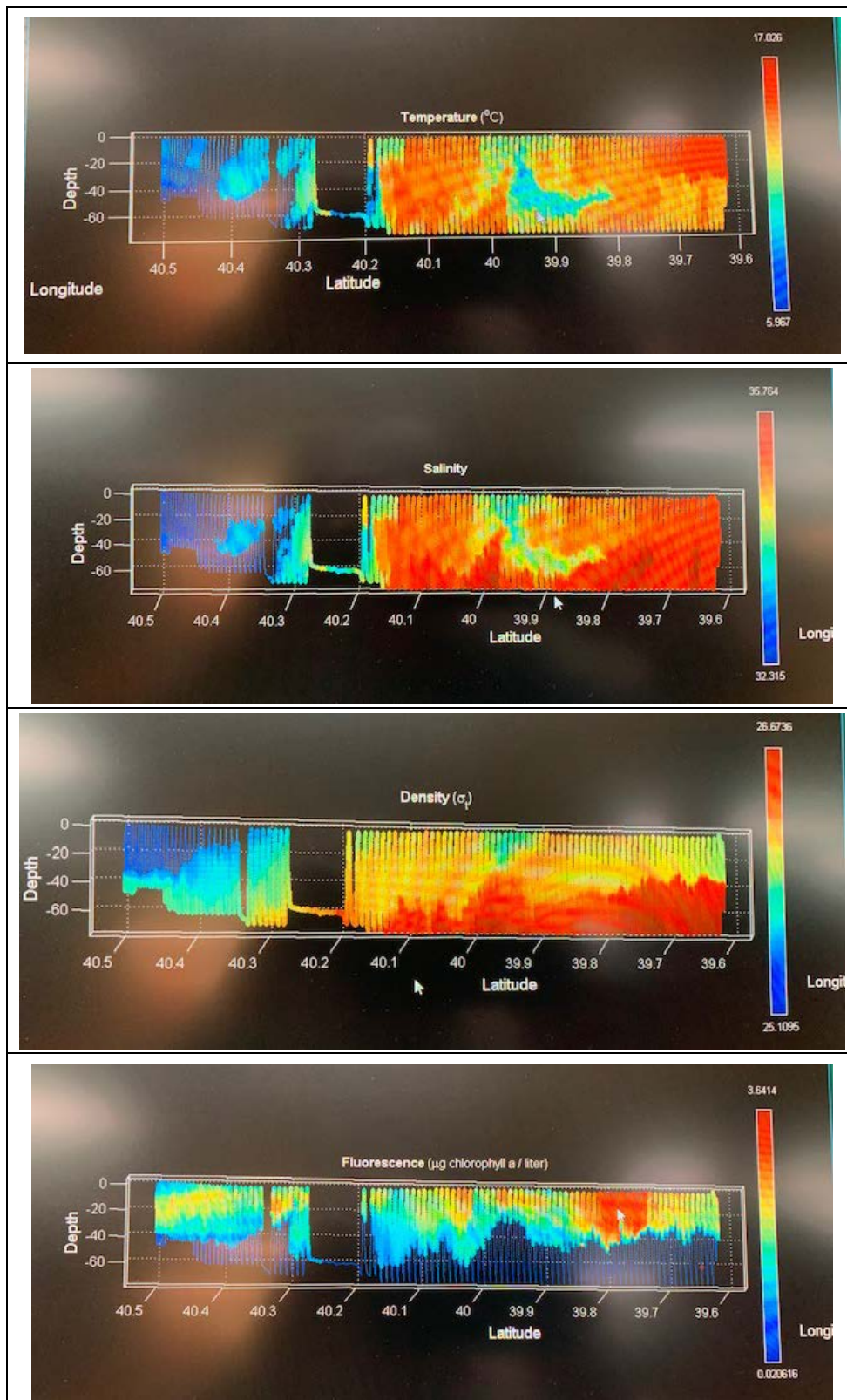


Figure 0514.1. May 14 VPR survey A5-A18.

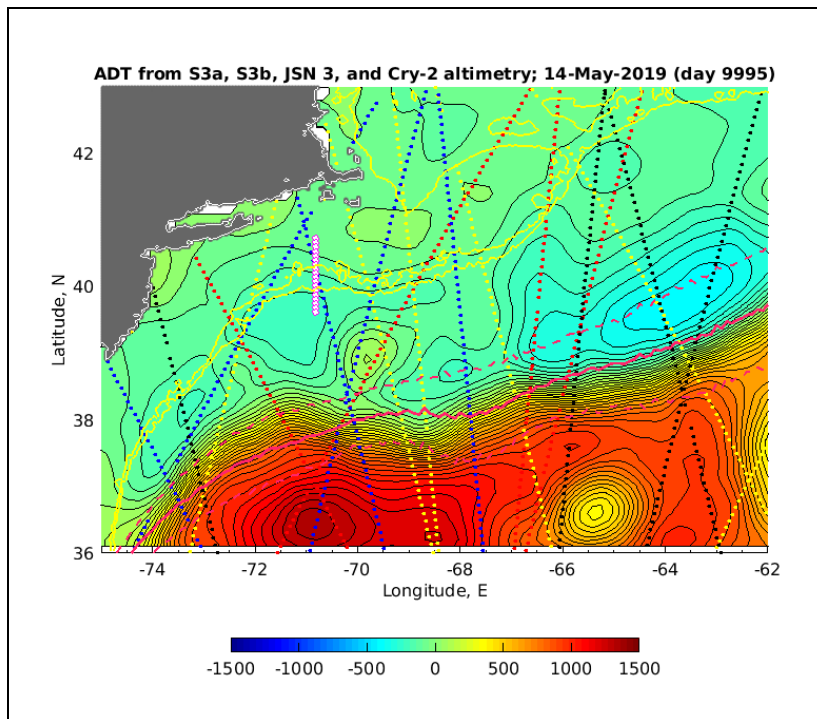


Figure 0515.1. Satellite altimetric analysis for 15 May 2019.

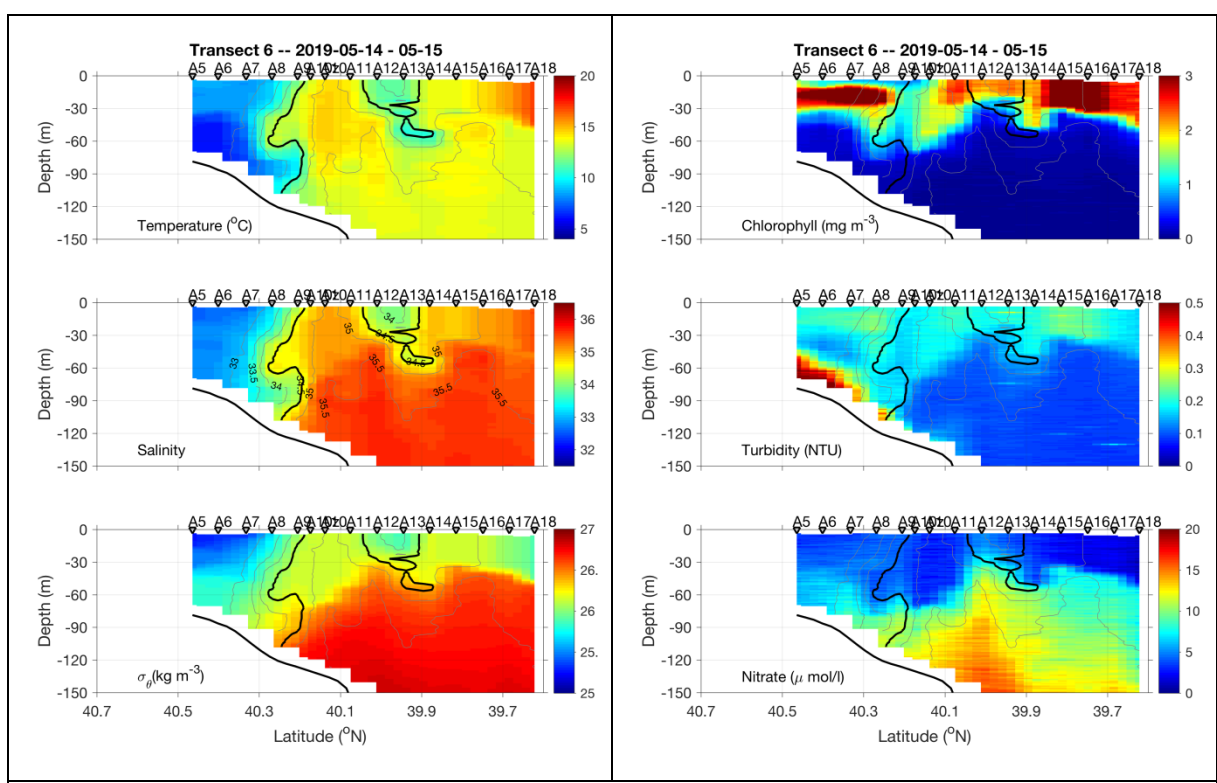


Figure 0515.1. May 14-15 section.

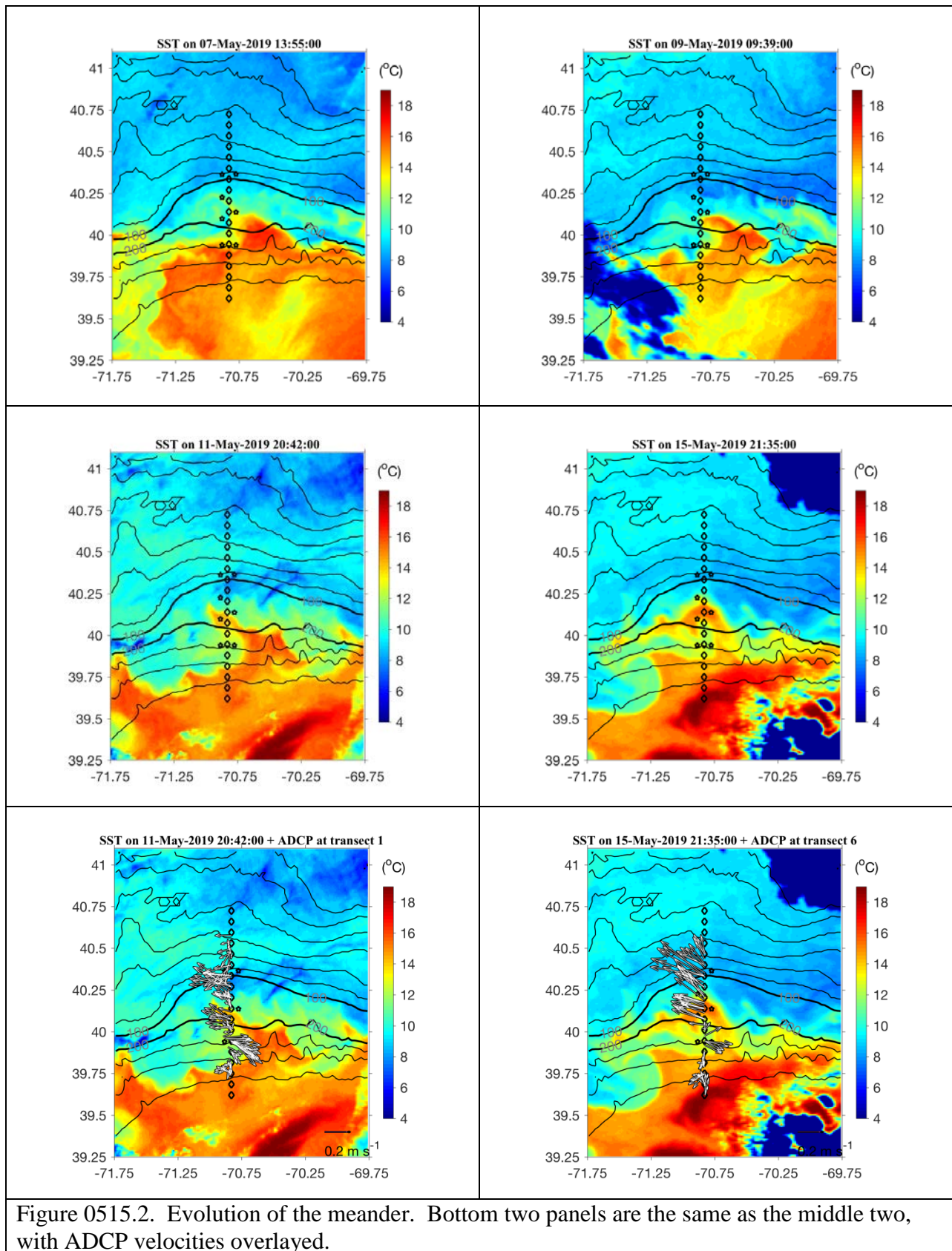


Figure 0515.2. Evolution of the meander. Bottom two panels are the same as the middle two, with ADCP velocities overlaid.

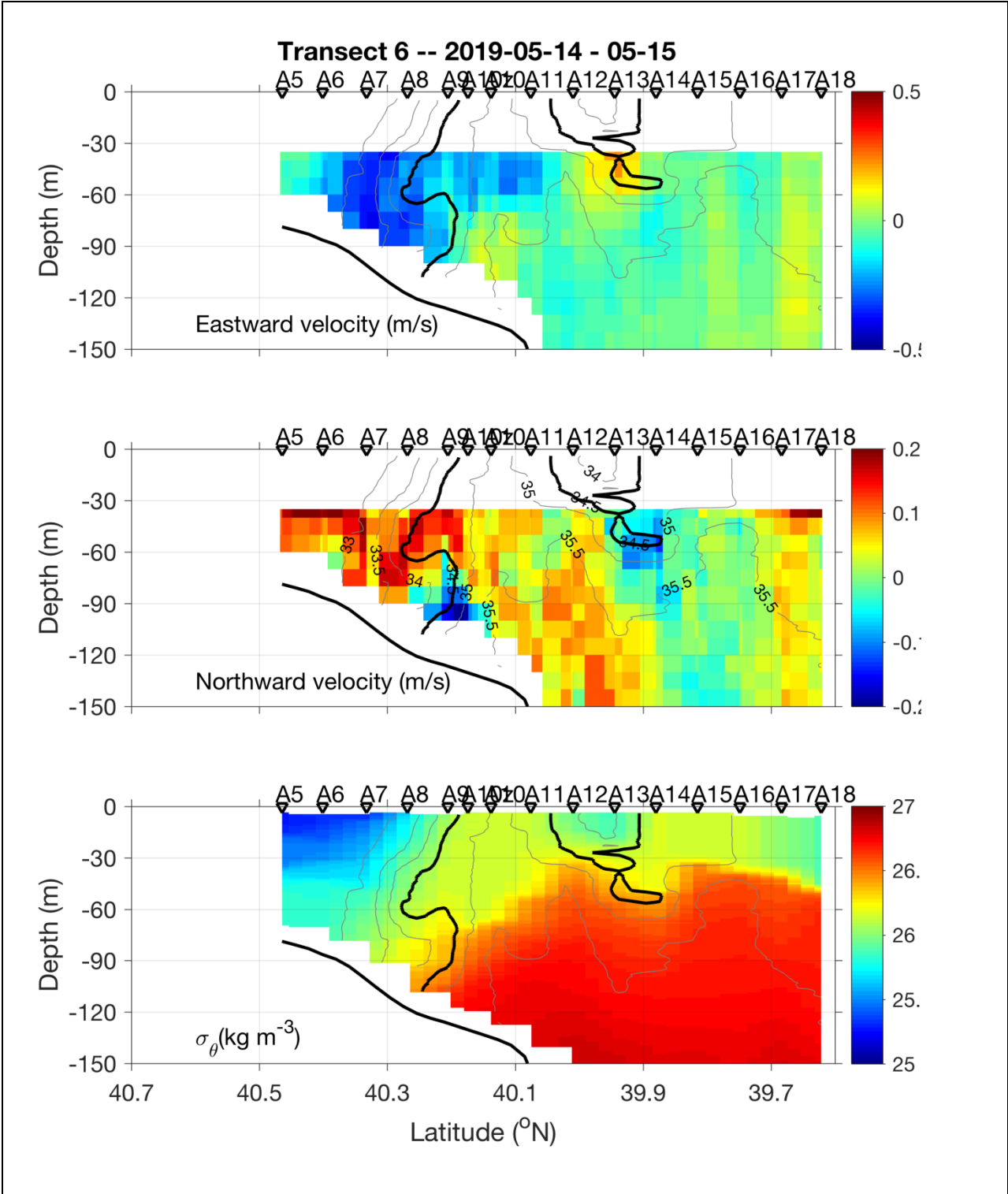


Figure 0515.3. Eastward and northward ADCP velocities (top two panels) and density (lower panel). Salinity contours overlaid on all three.

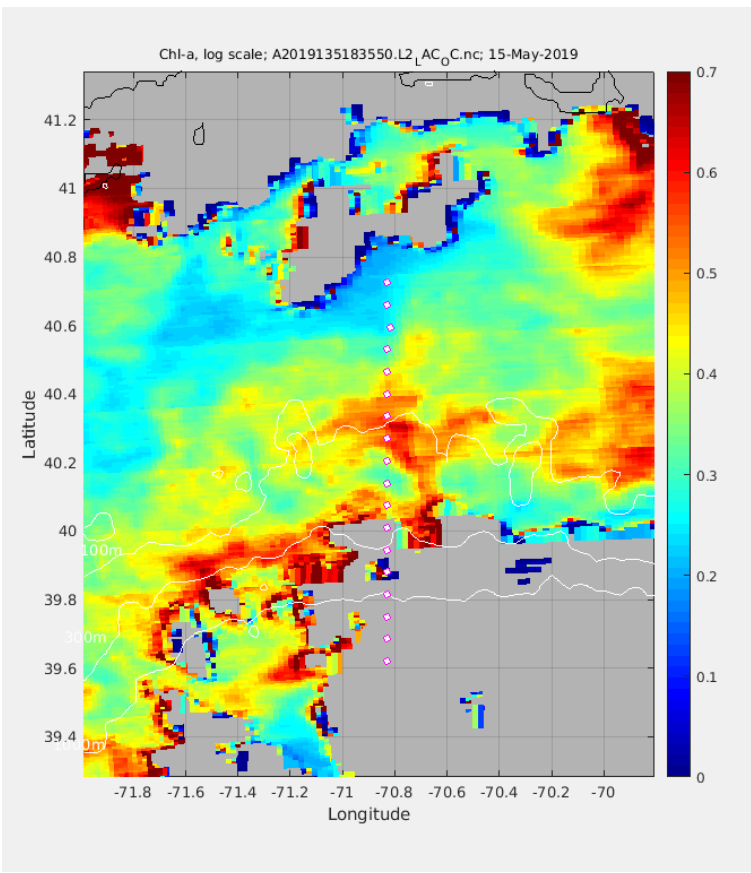


Figure 0515.4. MODIS chlorophyll image for 15 May 2019.

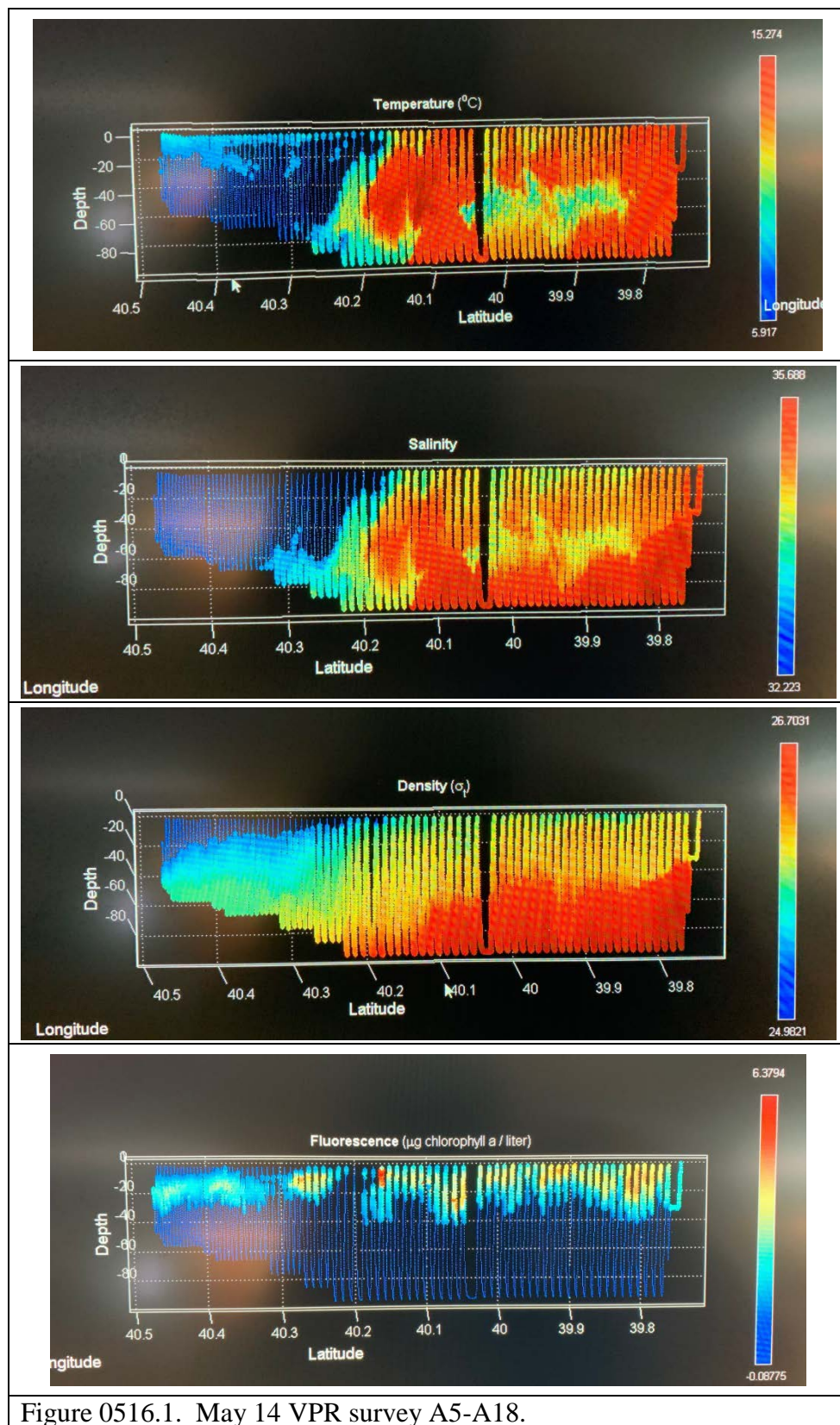


Figure 0516.1. May 14 VPR survey A5-A18.

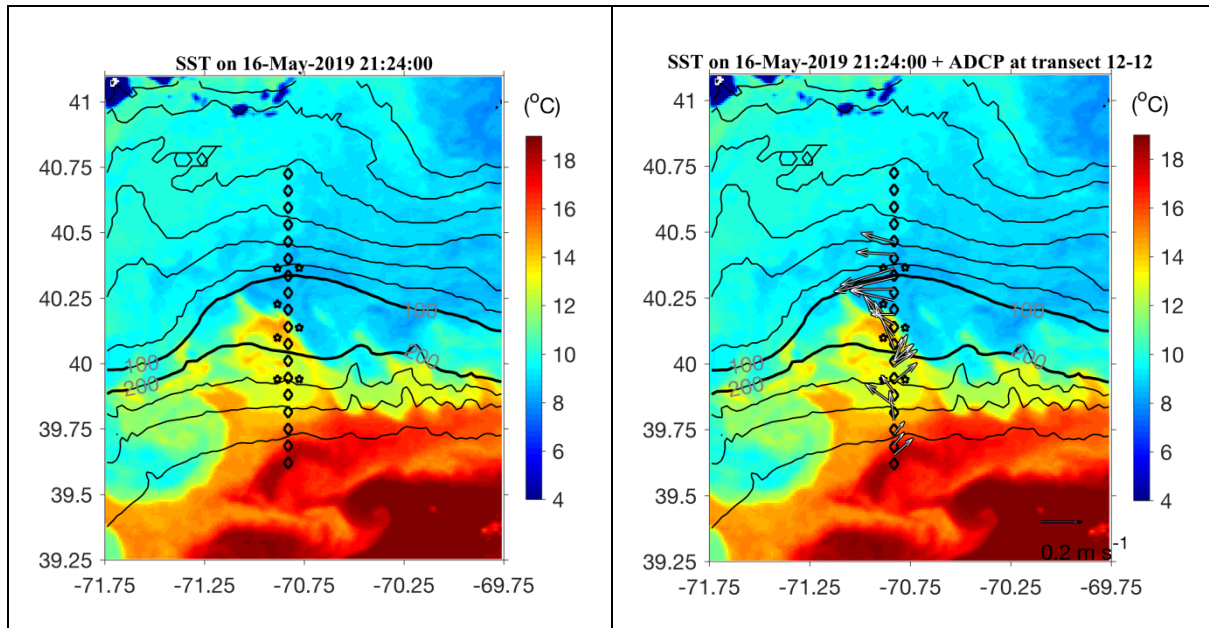


Figure 0516.2. SST imagery for May 16 with and without ADCP velocity overlaid.

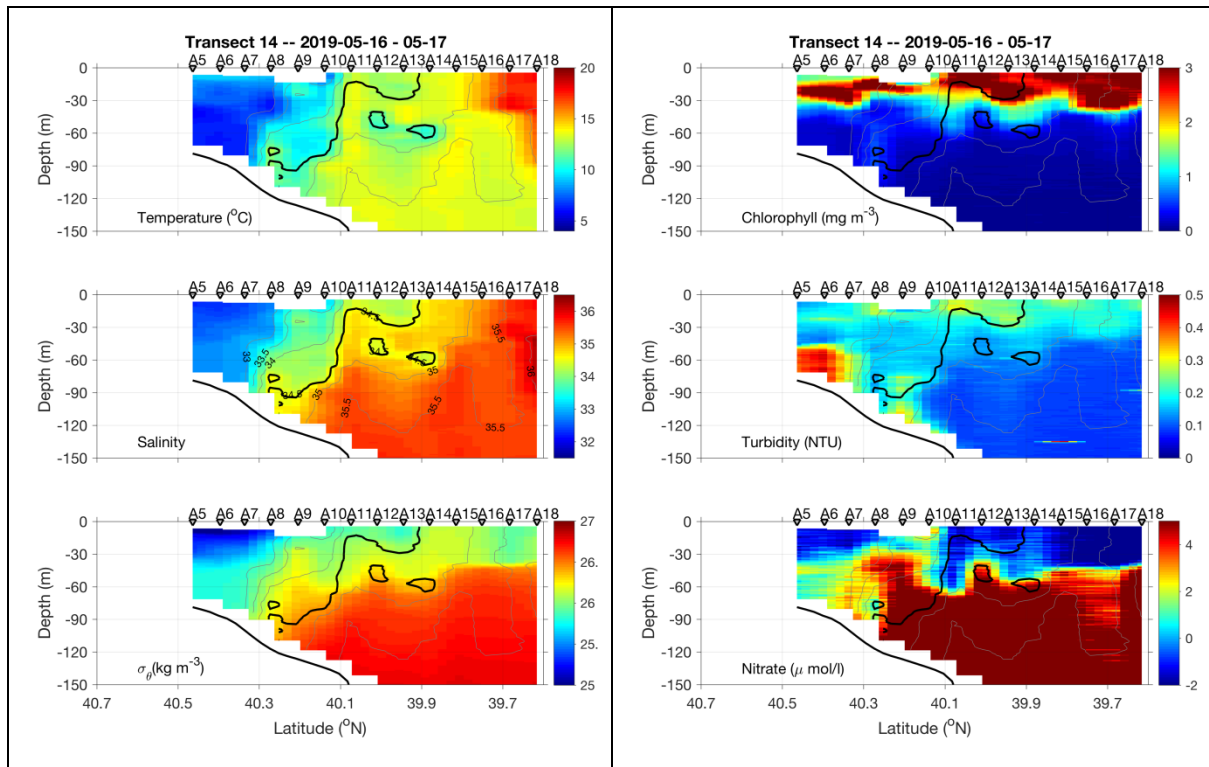


Figure 0517.1. May 16-17 section.

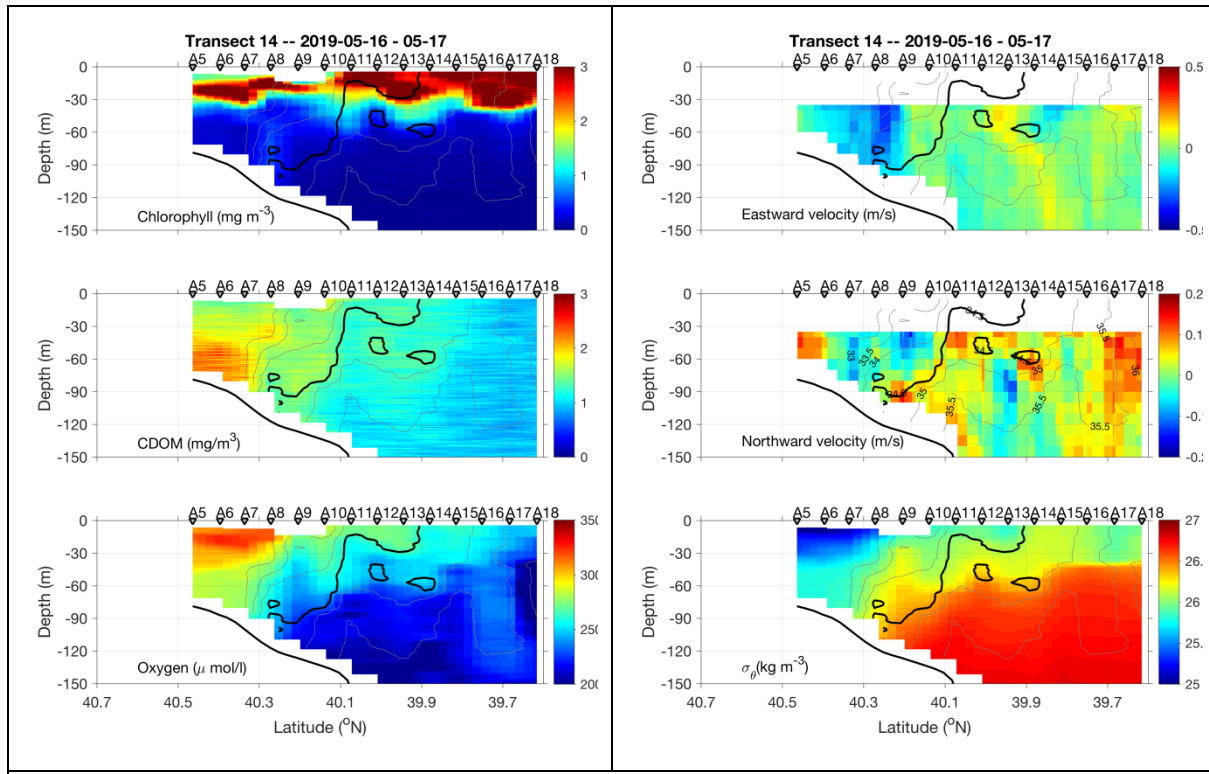
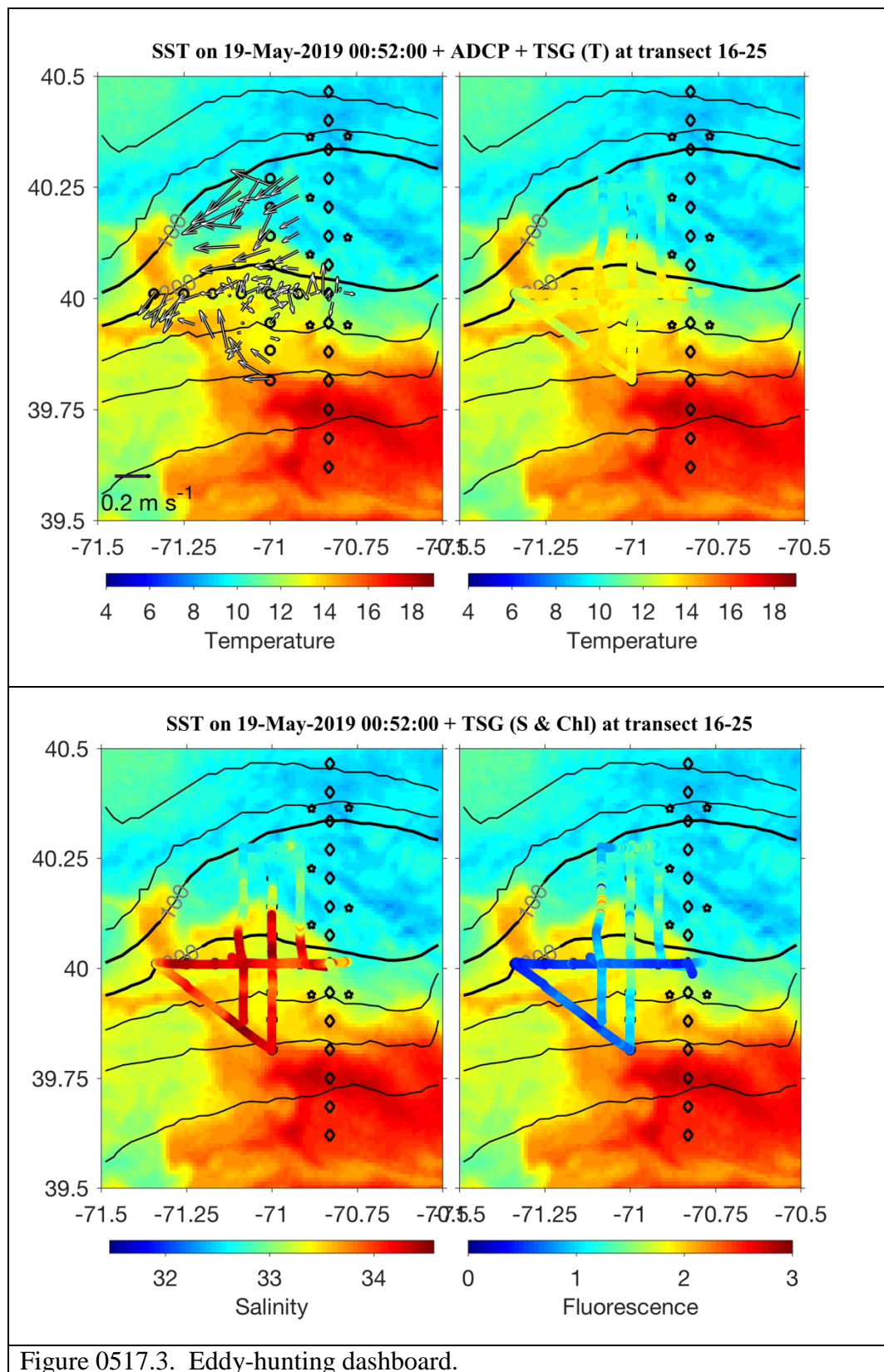


Figure 0517.2. May 16-17 section.



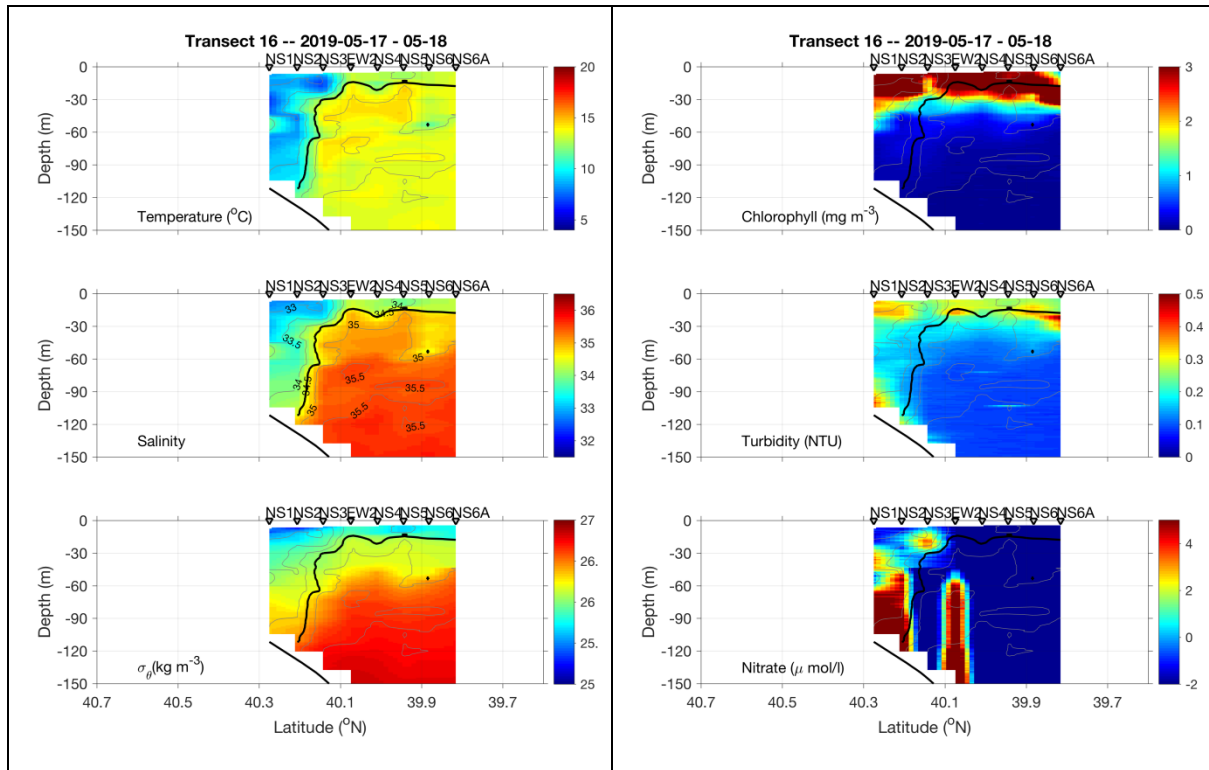


Figure 0518.1. N-S Eddy section, 17-18 May.

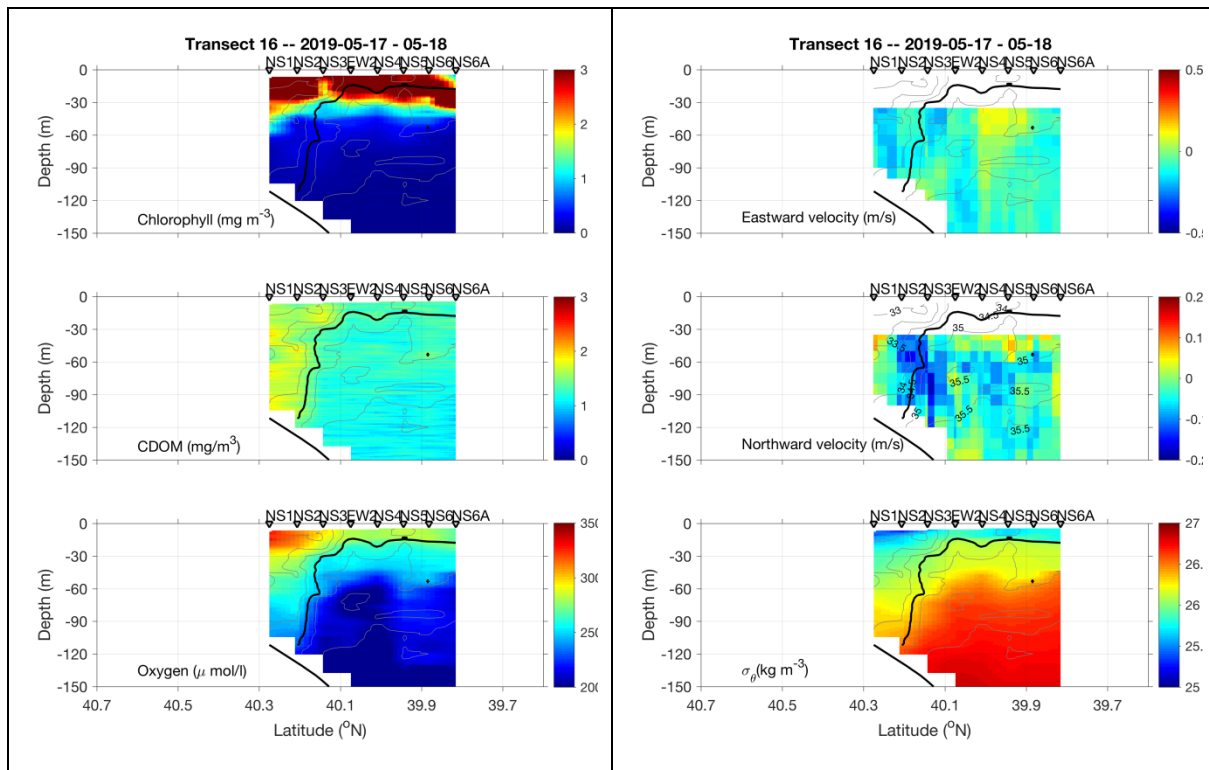


Figure 0518.2. N-S Eddy section, 17-18 May.

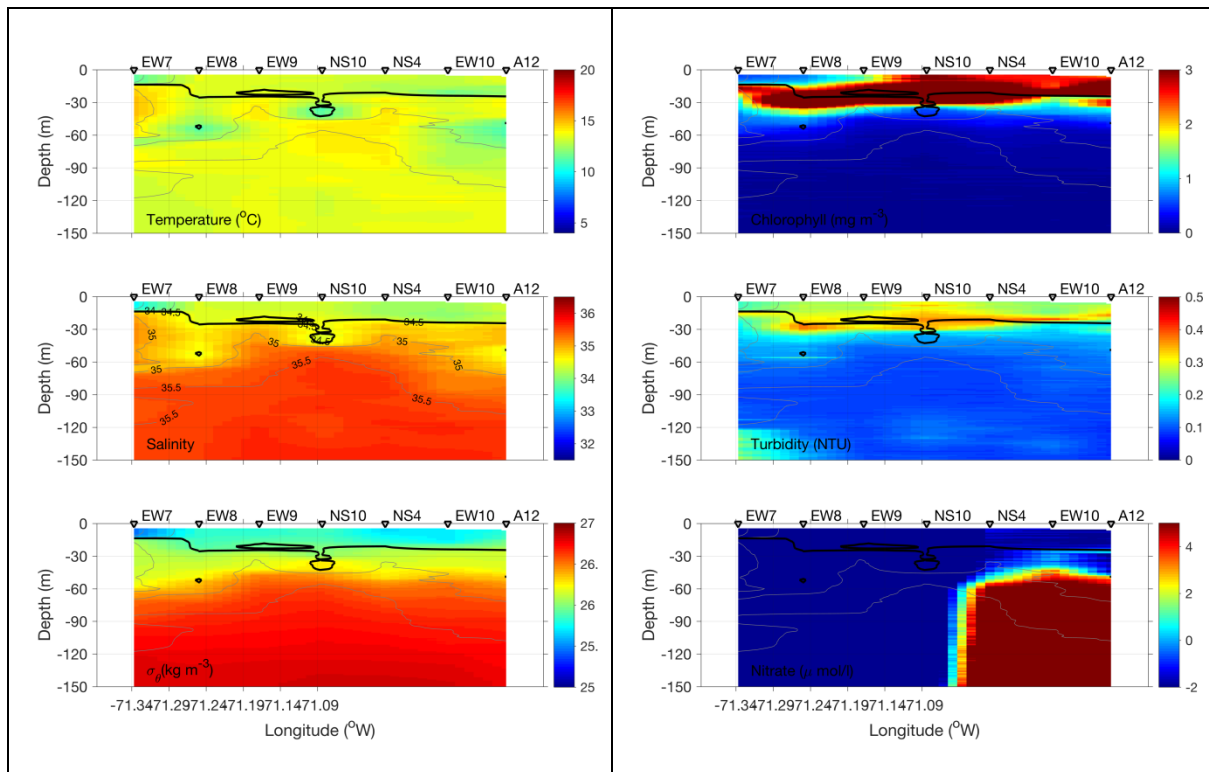


Figure 0518.3. EW Eddy section, 18 May.

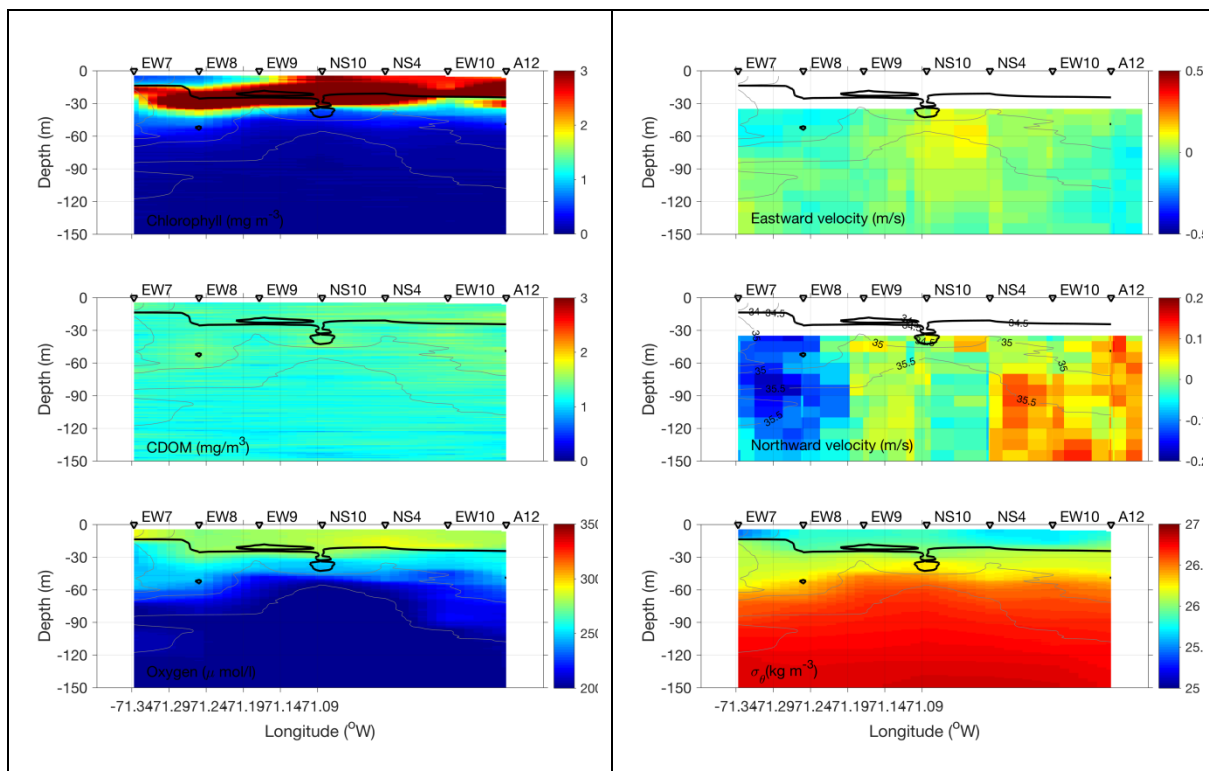


Figure 0518.4. EW Eddy section, 18 May.

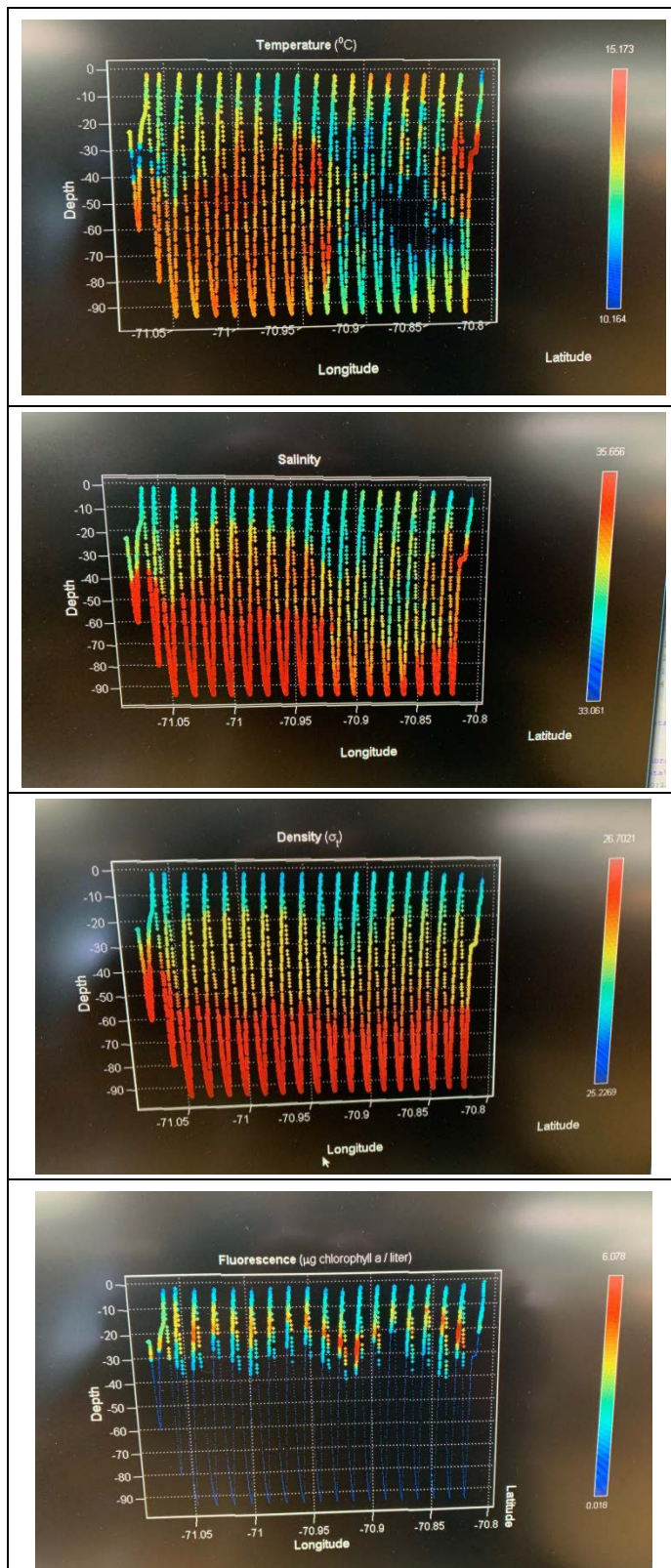


Figure 0518.5. Radial VPR survey from eddy center (NS10) to the edge (A12) on May 18.

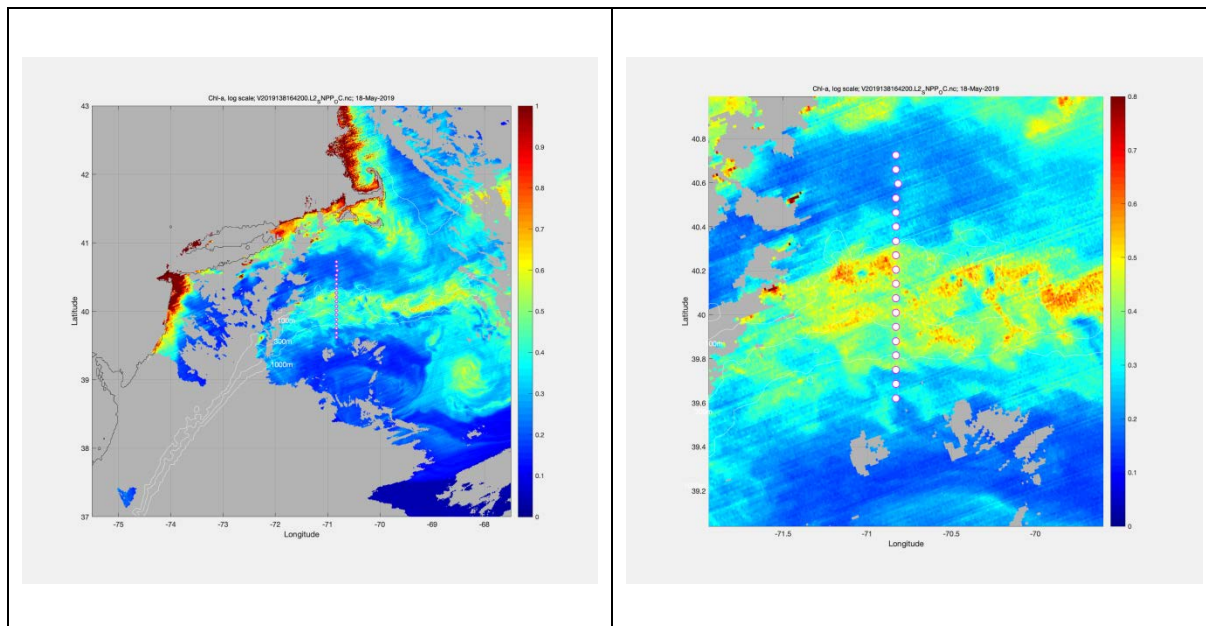


Figure 0519.1. VIIRS chlorophyll for 18 May: regional (left) and zoom (right).

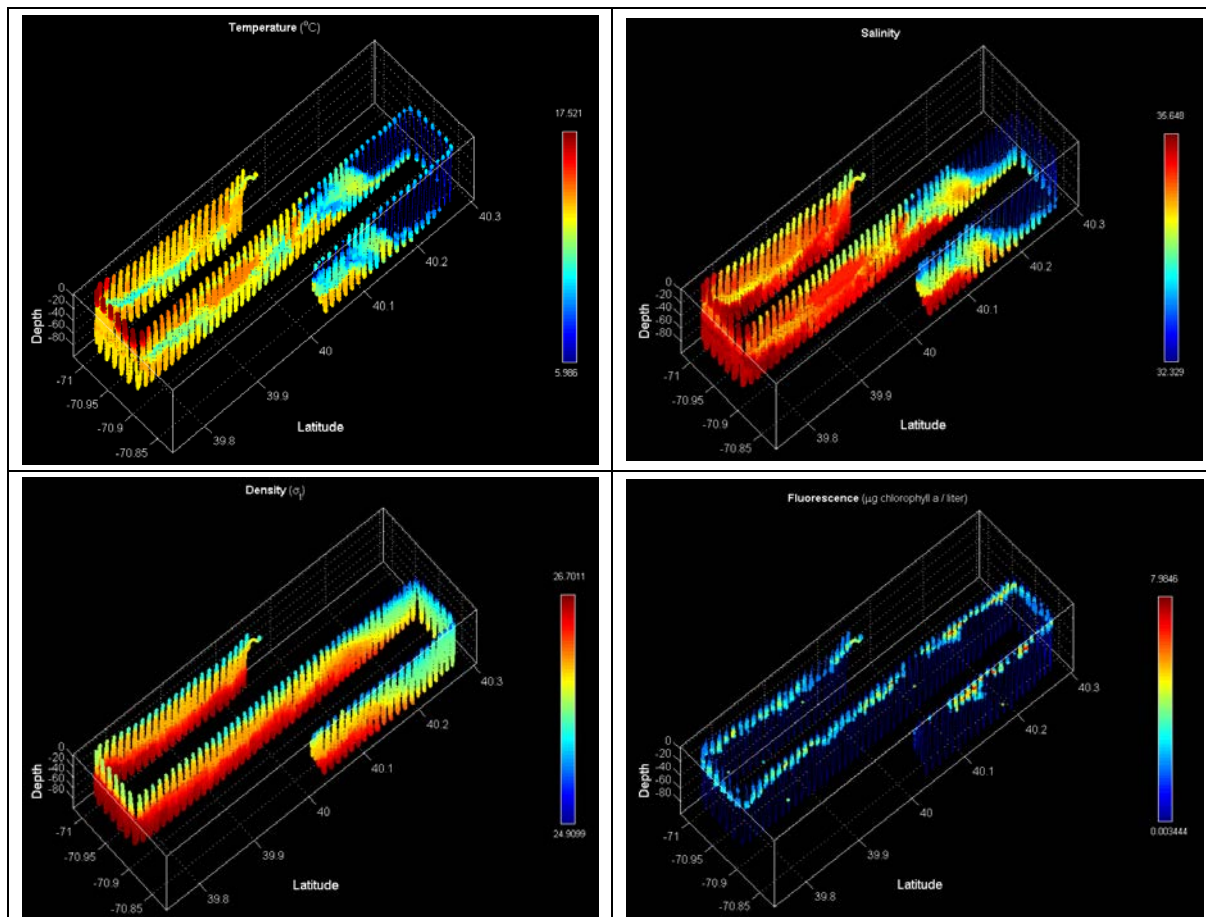


Figure 0519.2. VPR survey on May 19.

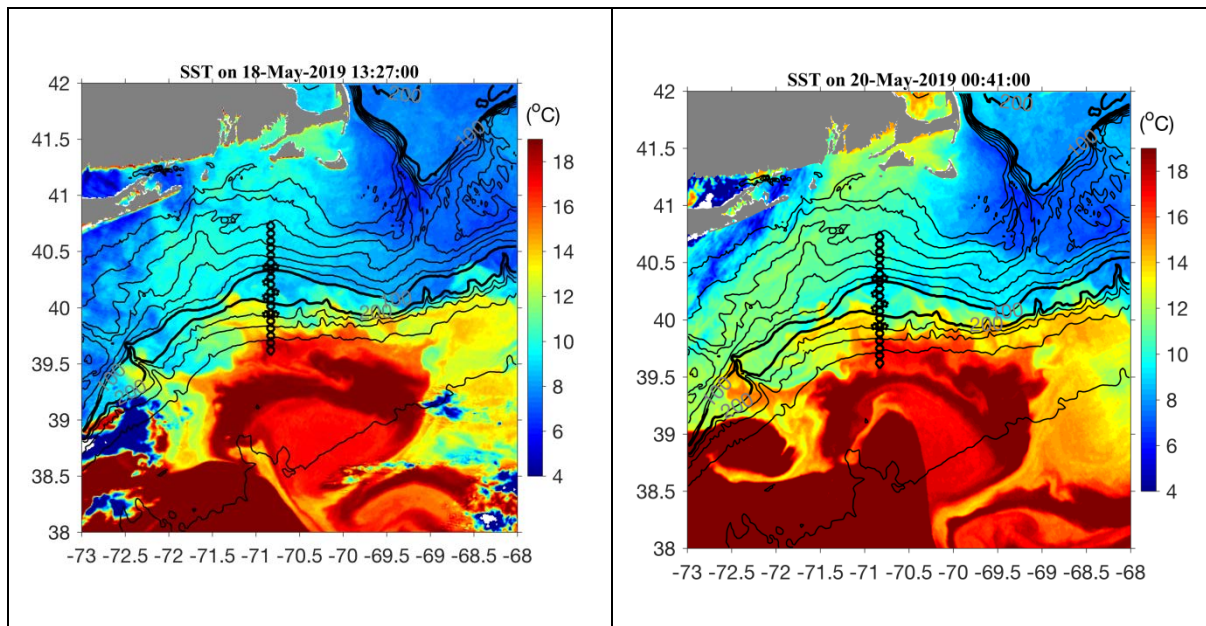


Figure 0519.3. SST imagery for May 18 and 20.

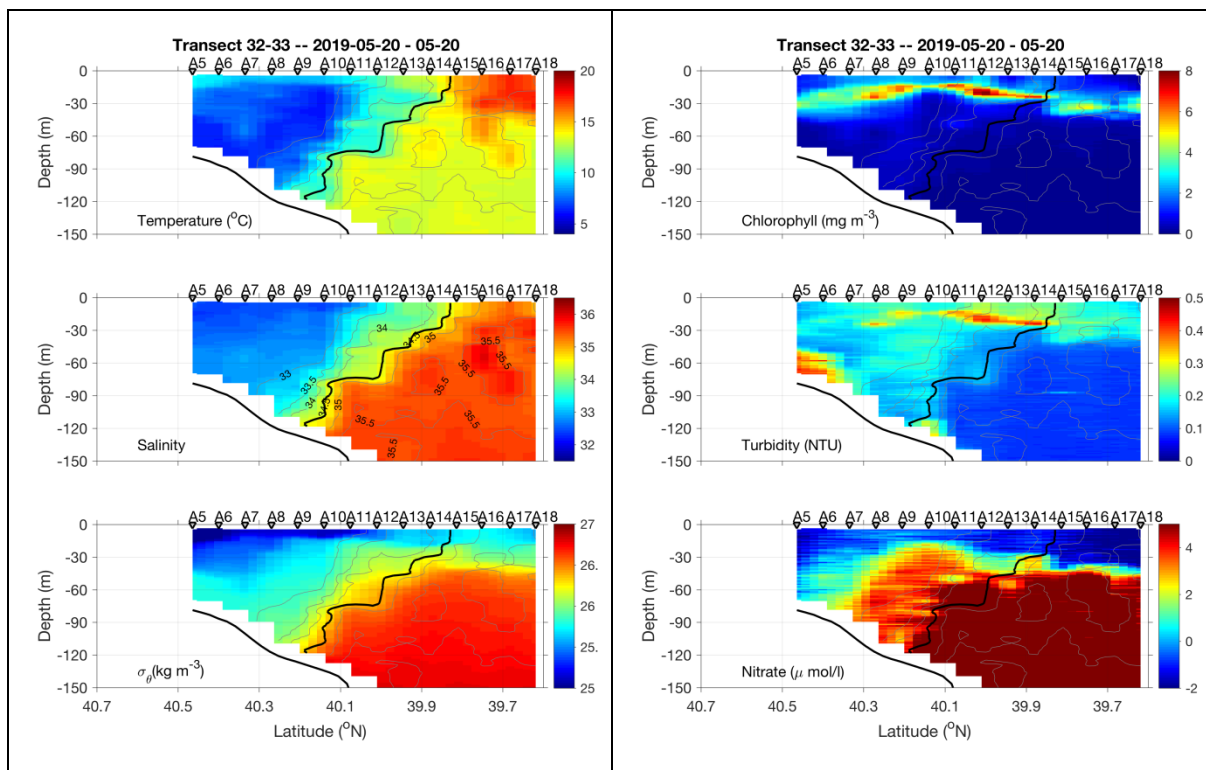


Figure 0520.1. May 19-20 section.

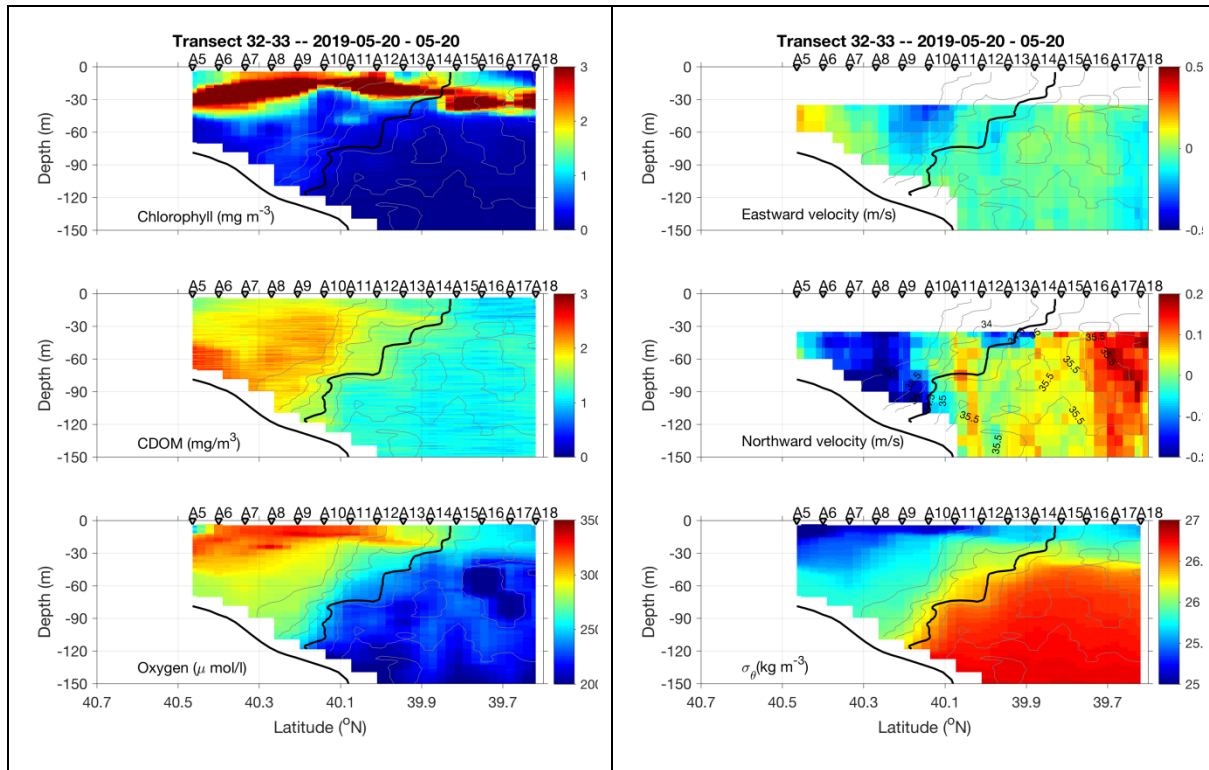


Figure 0520.2. May 19-20 section.

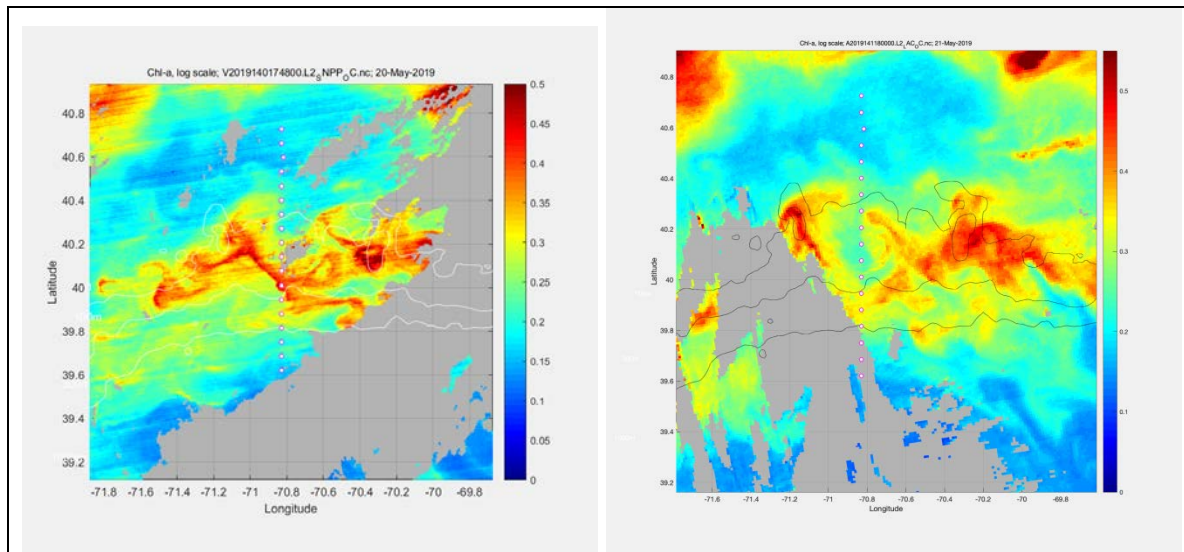


Figure 0520.3. VIIRS image for May 20 and 21; note slightly different colorbar.

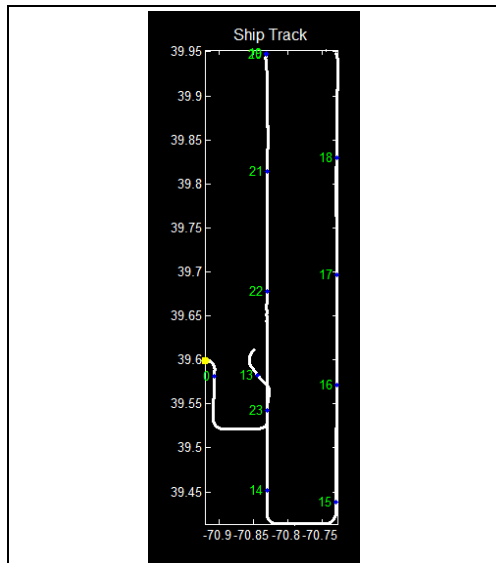


Figure 0521.1. VPR surveys 5 and 6 combined. VPR5 began at A18 (ca. 1300 hours), transited south, turned east, and ran back north to the latitude of A13. VPR6 began at A13 (ca. 2000 hours), transited south to join the prior leg, turned west, then north.

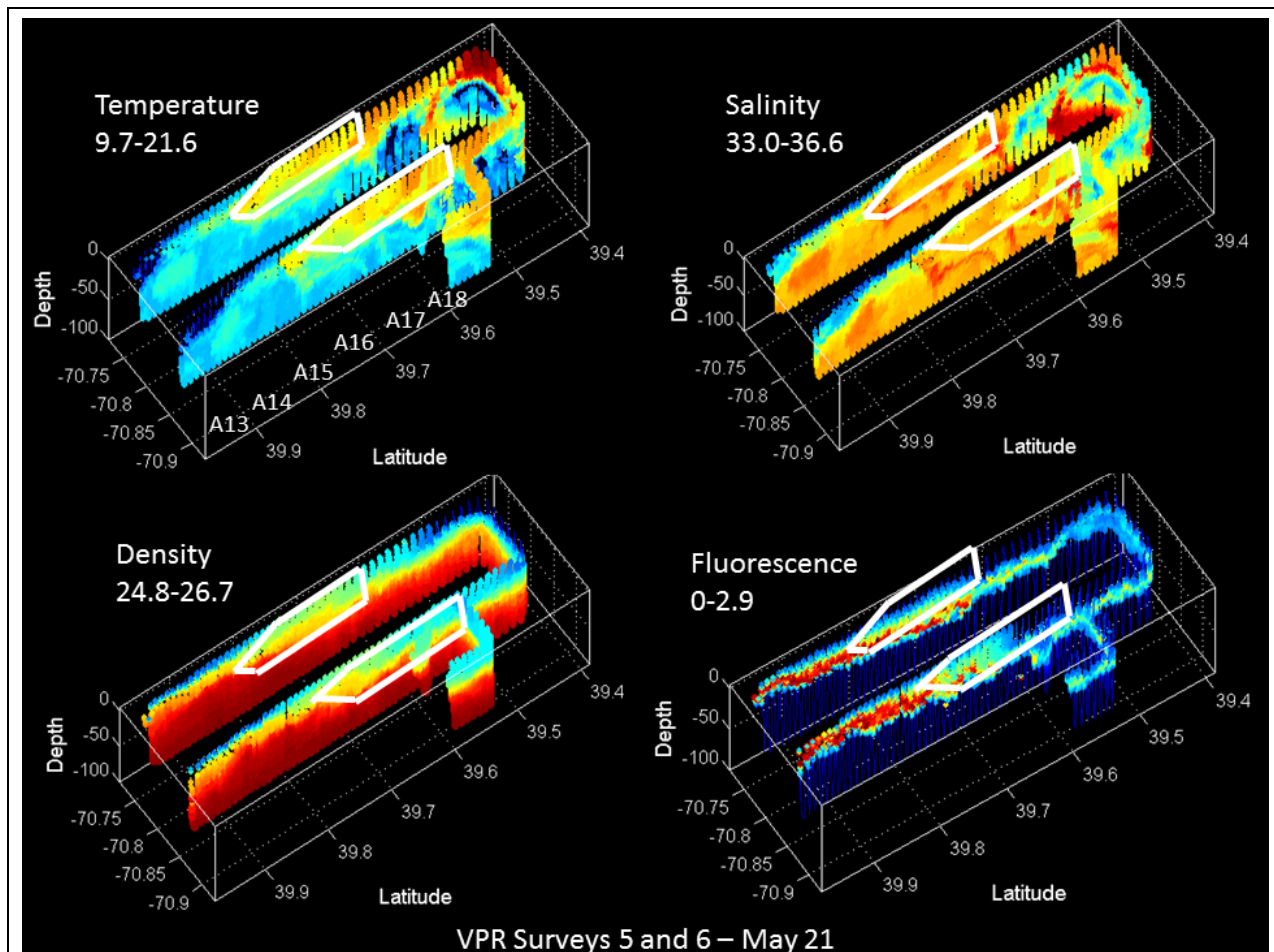
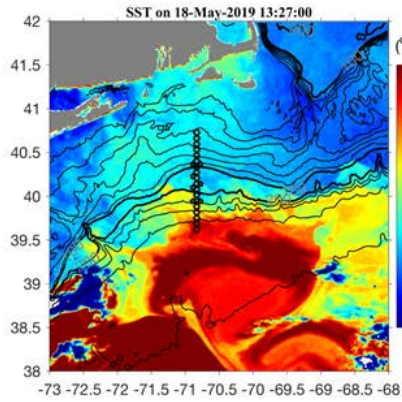


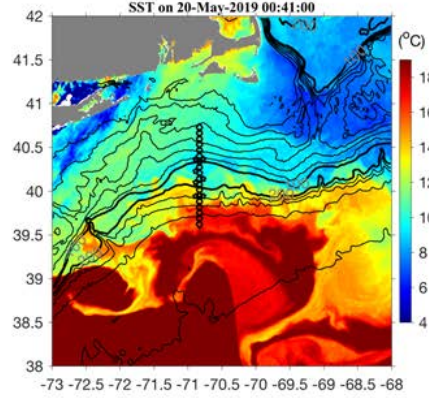
Figure 0521.2. VPR surveys 5 and 6. Region of highest abundance of rod-shaped diatoms is indicated by white polygons.

SST

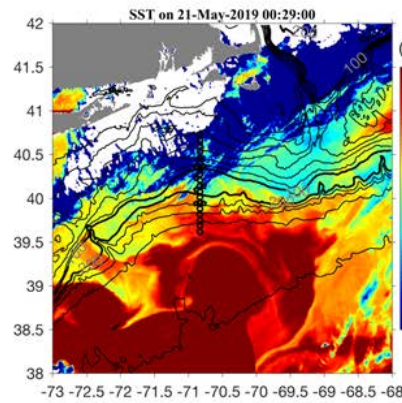
May 18



May 20



May 21



May 22

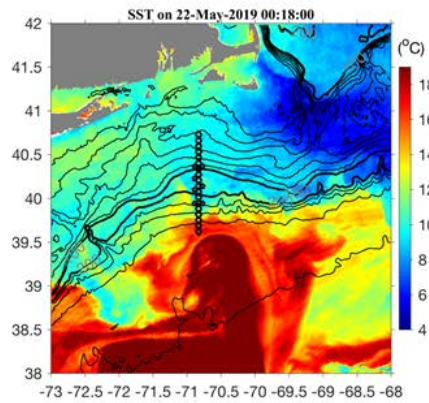


Figure 0521.3. SST imagery for May 18, 20, 21, and 22.

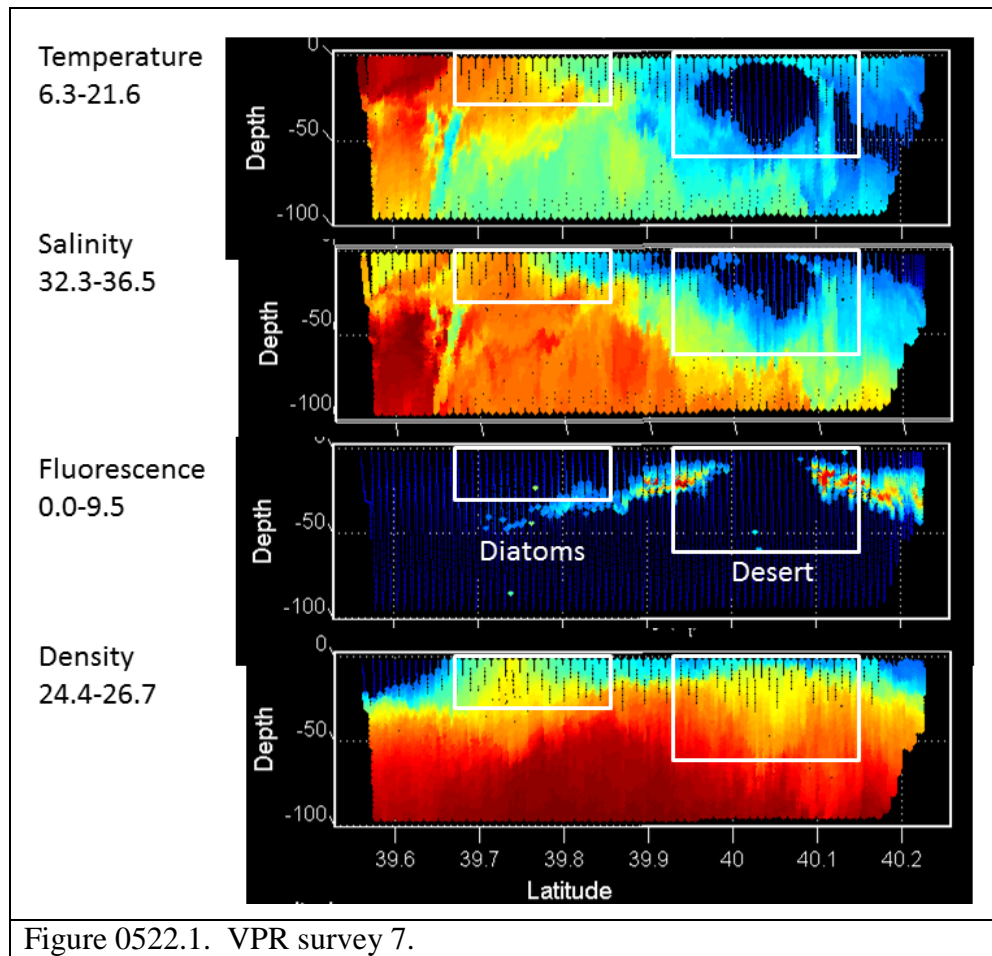


Figure 0522.1. VPR survey 7.

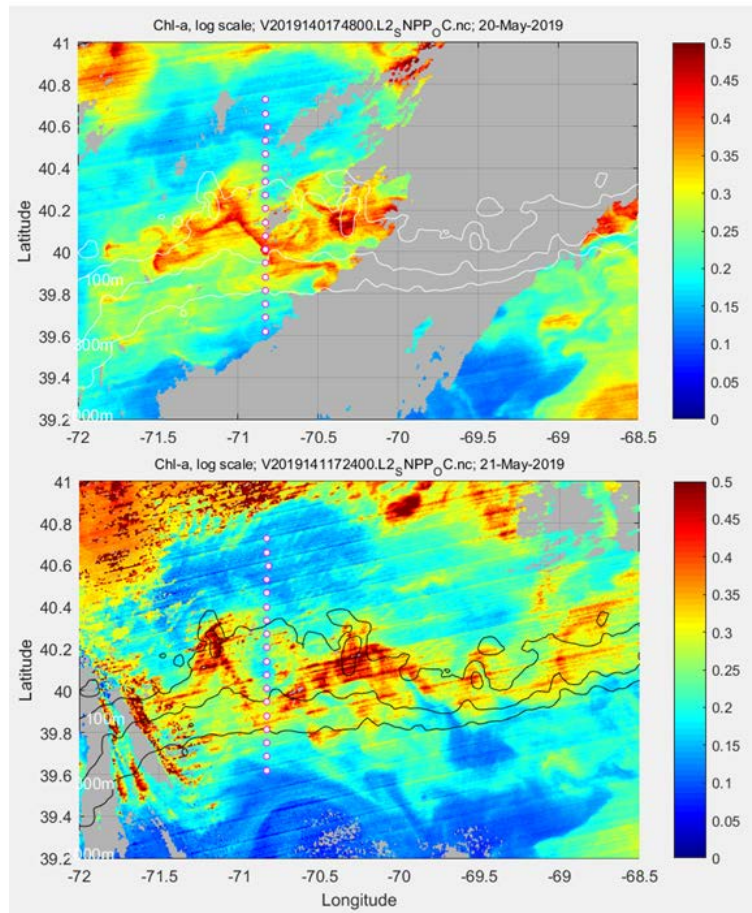


Figure 0522.2. VIIRS chlorophyll images for May 20 (top) and May 21 (bottom).

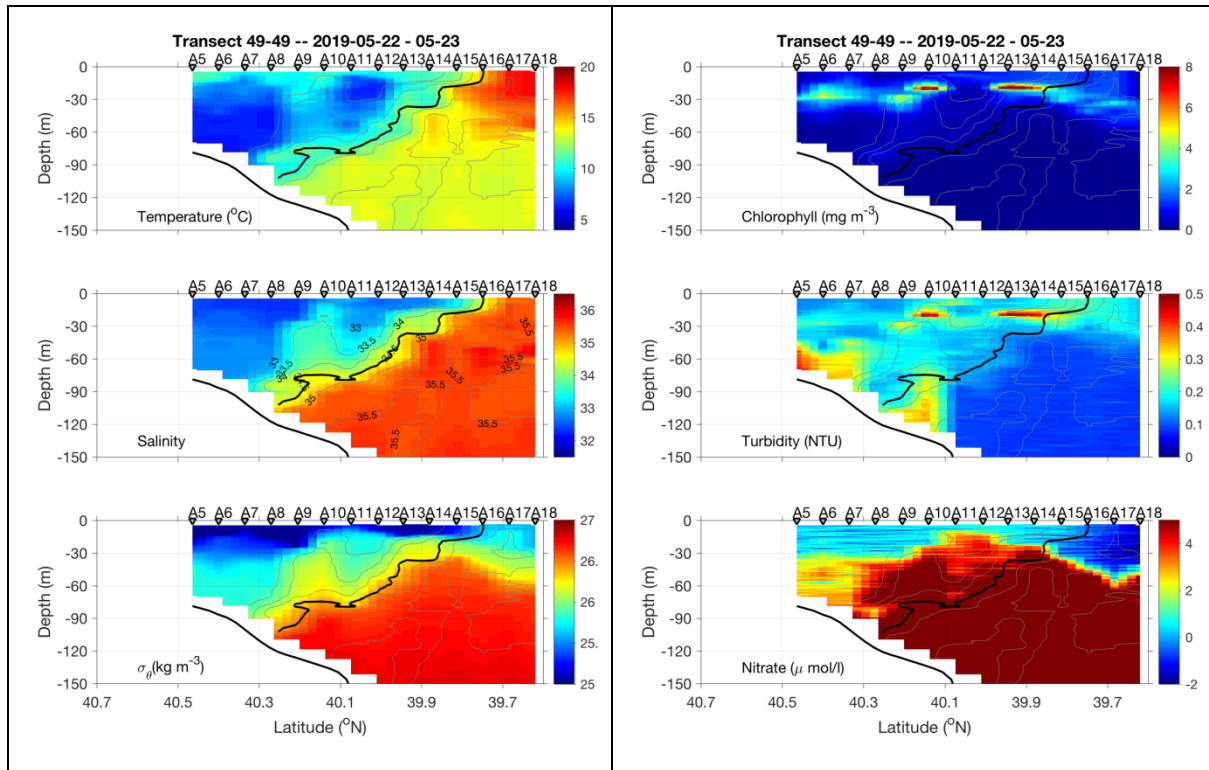


Figure 0523.1. May 22-23 section.

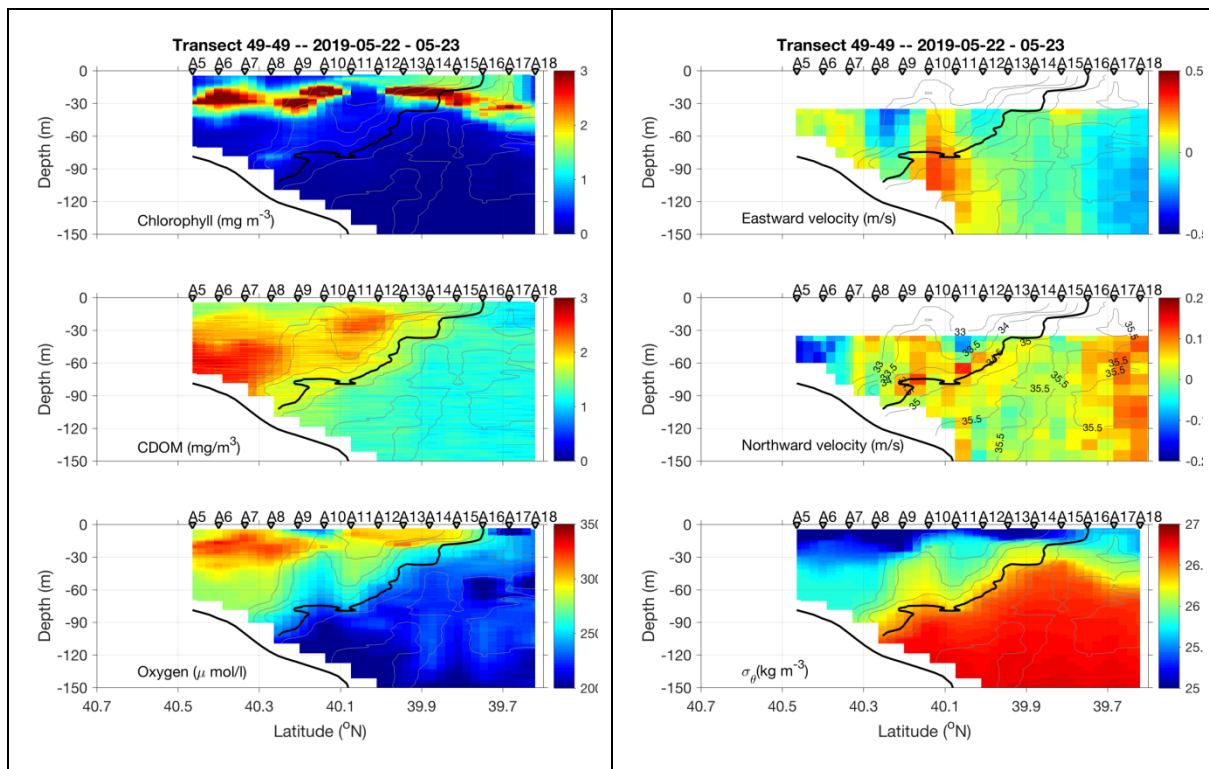


Figure 0523.2. May 22-23 section.

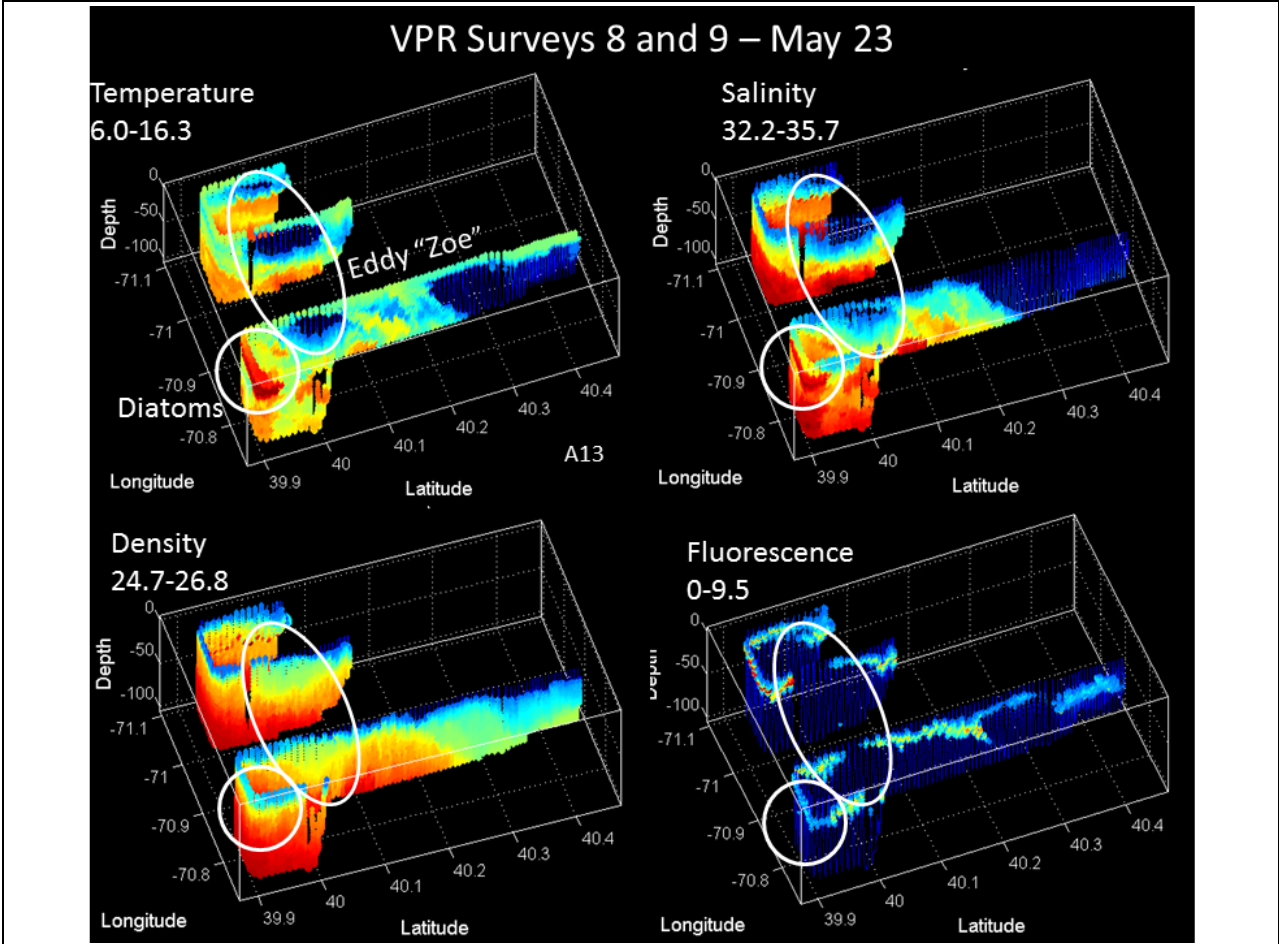


Figure 0523.3. VPR survey on May 23.

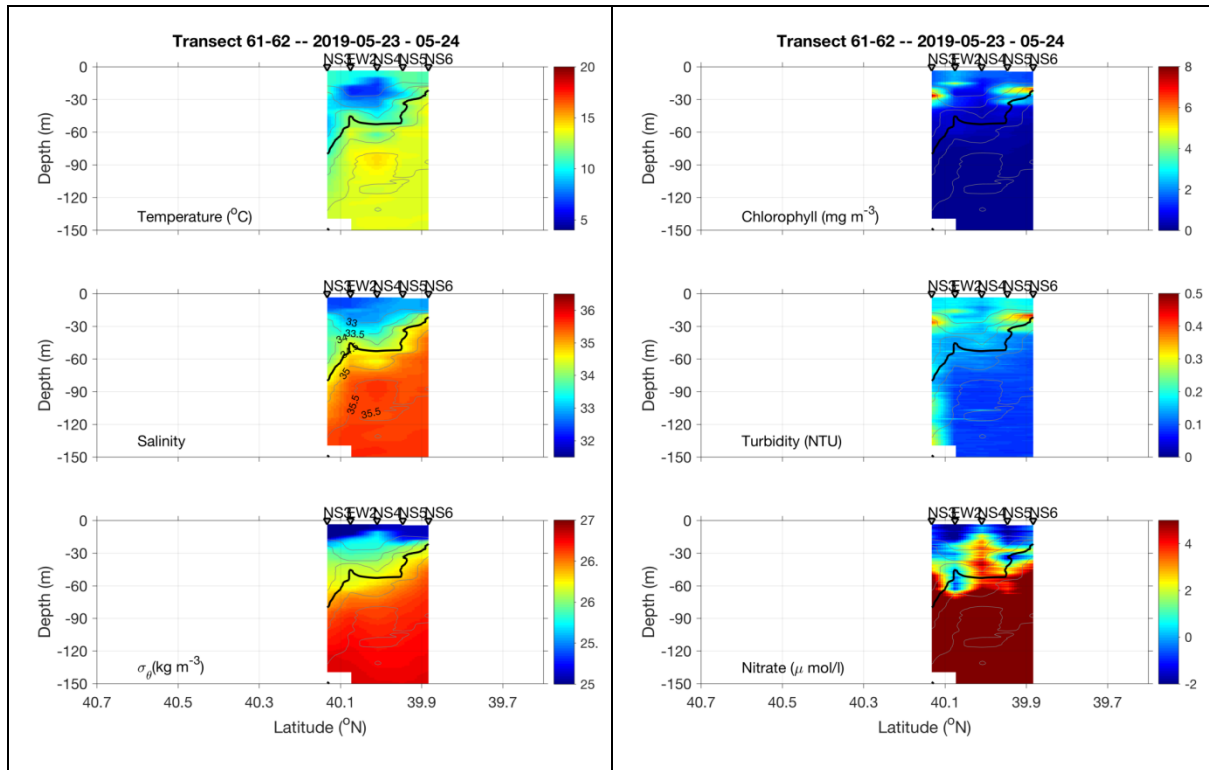


Figure 0524.1. May 23-24 eddy survey.

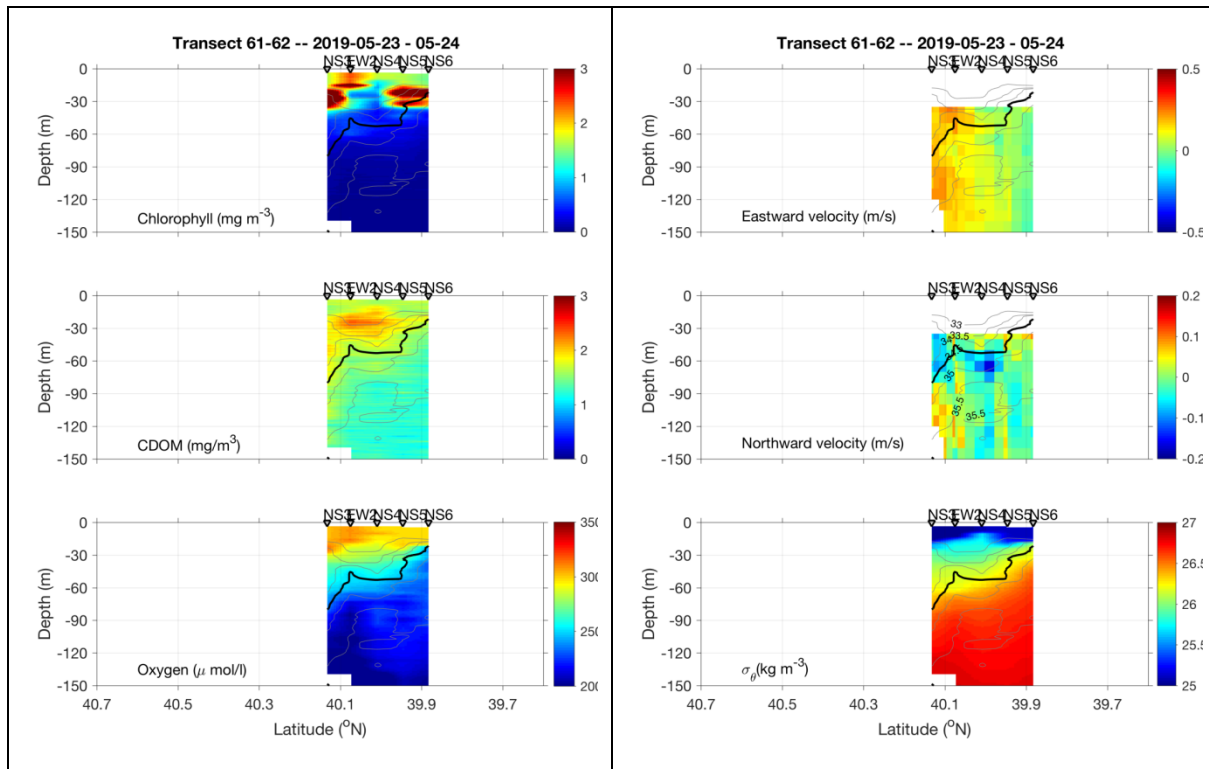


Figure 0524.2. May 23-24 eddy survey.

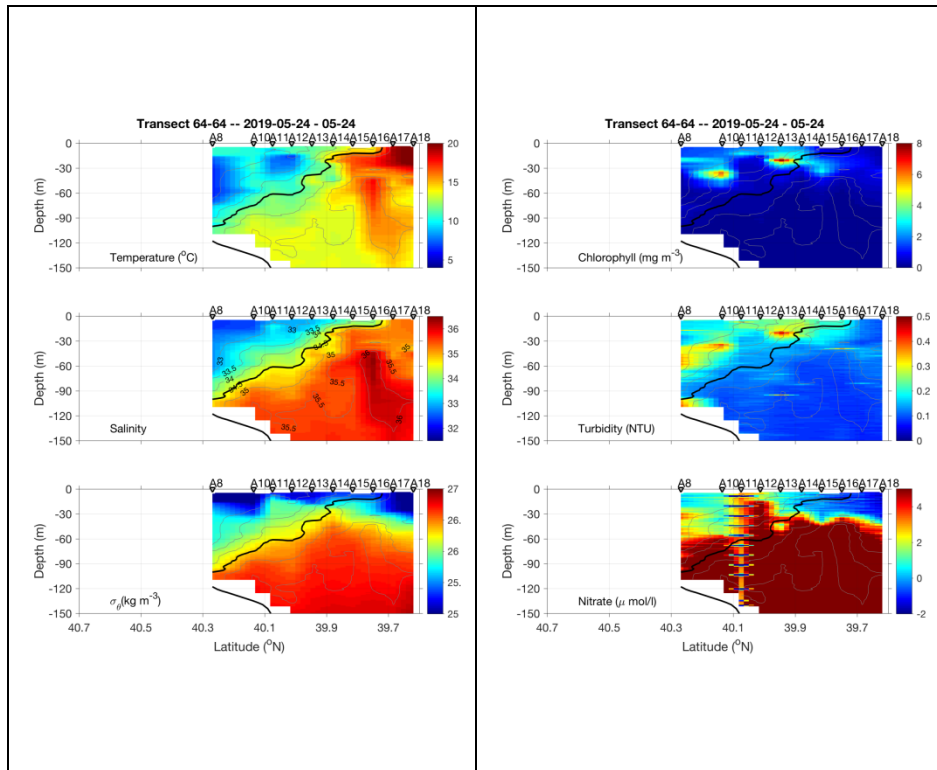


Figure 0524.3. May 24 final transect.

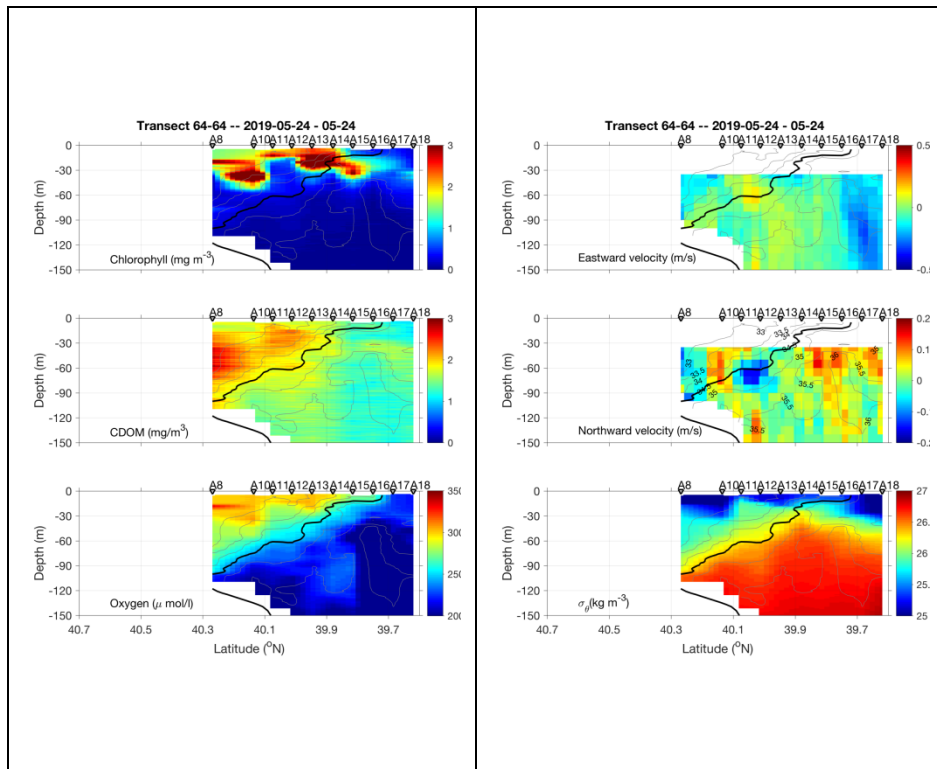


Figure 0524.4. May 24 final transect.

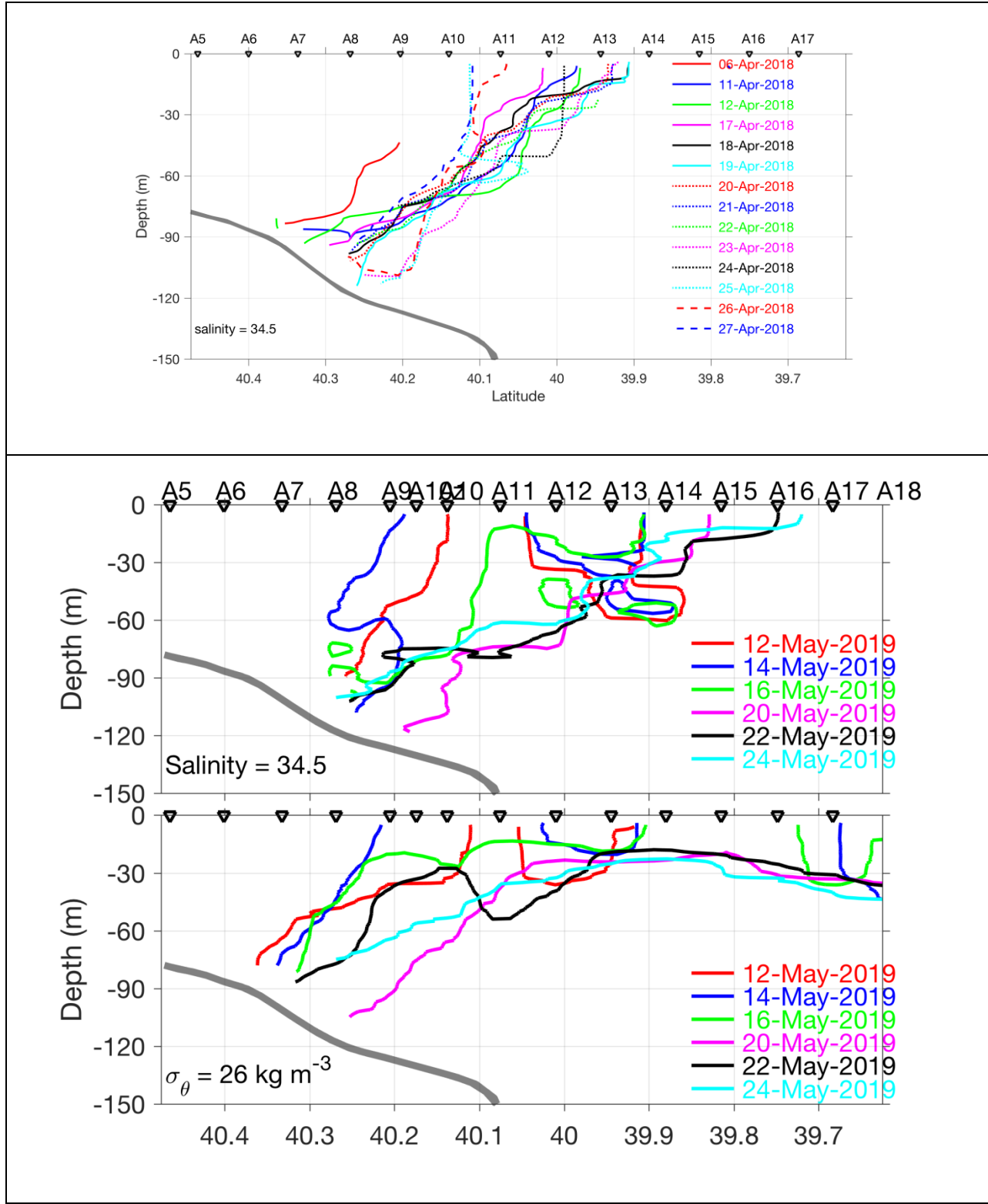


Figure 0525.1: Frontal positions for AR29 (top) and RB1904 (bottom).

